Unequal Thermal Risks in a Socioeconomically Important Tropical Reef Fishery

Andrew R. Villeneuve[1], Merrill Baker-Médard[2], Bemahafaly Randriamanantsoa[3], Easton R. White[1]

[1]Department of Biological Sciences, University of New Hampshire, NH, USA

[2]Department of Environmental Studies, Middlebury College, Middlebury, VT, USA

[3]Wildlife Conservation Society Madagascar Program, Soavimbahoaka, Antananarivo 101, Madagascar

ORCID: Andrew Robert Villeneuve: 0000-0001-7303-5931; Merrill Baker-Médard: 0000-0002-3724-8320; Easton Radley White: 0000-0002-0768-9555

Keywords: marine microclimate, marine heatwaves, fisheries climate sensitivity, Western Indian Ocean, reef flats, gleaning

Author Contributions

Conceptualization: ARV, ERW; Methodology: ARV, MBM, BR, ERW; Formal Analysis: ARV; Writing - first draft: ARV; Writing - review and editing: ARV, MBM, BR, ERW; Funding Acquisition: MBM, ERW; Project Administration: MBM, BR, ERW.

Statements and Declarations

The authors declare no competing interests.

Abstract

1. Climate change poses an understudied threat to the coastal reef systems of the Western Indian Ocean (WIO), a biodiversity hotspot critical for the maintenance of subsistence fisheries. The southwestern coast of Madagascar is especially sensitive to disturbances due to the high level of socioecological dependence on functioning reefs.
2. Fishing in this region is spatially structured. For example, gleaning (pêche-à-pied) is undertaken predominantly by women and children walking in intertidal reef flat and crest habitats during low tide, while boat-based fishing occurs across a range of reef geomorphic zones. These zones may experience different microclimates due to differences in depth, water residence time, and oceanic exposure.
3. To characterize the thermal microclimates of these zones, we deployed temperature loggers for over a year across reef geomorphic zones on Salary Reef, Madagascar. We further examined modeled tide elevation data over the deployment period and the 18.6-year tidal cycle.
4. Subtidal loggers showed similar mean temperature but diverged up to 27% in cumulative hours above 30 °C. Compared with gridded temperature datasets, logger observations revealed higher extremes and lower minima, underscoring the added fidelity of in-situ measurements.
5. The intertidal logger recorded extreme thermal stress (up to 48.8 °C) in gleaning habitats, with maximum heat events occurring in transitional “shoulder” seasons rather than peak summer. Tidal analyses showed that midday low tides in these transitional periods drive extreme intertidal warming.
6. Fisheries in Madagascar will likely experience uneven and seasonally distinct thermal risks. Climate adaptation must consider how microclimate variability mediates socioecological vulnerability in coastal oceans.

Résumé

1. Le changement climatique représente une menace encore peu étudiée pour les systèmes récifaux côtiers de l'océan Indien occidental (OIO), un hotspot de biodiversité essentiel au maintien des pêches de subsistance. La côte sud-ouest de Madagascar est particulièrement sensible aux perturbations en raison de la forte dépendance socio-écologique à des récifs fonctionnels.
2. Les pratiques de pêche dans cette région sont spatialement structurées. Par exemple, la pêche à pied (*gleaning*), pratiquée principalement par les femmes et les enfants, se déroule dans les habitats intertidaux de platiers et de crêtes récifales à marée basse, tandis que la pêche embarquée couvre un ensemble de zones géomorphologiques récifales. Ces zones peuvent présenter des microclimats distincts en fonction de la profondeur, du temps de résidence de l'eau et de leur exposition à l'océan ouvert.
3. Afin de caractériser ces microclimats thermiques, nous avons déployé des enregistreurs de température pendant plus d'un an dans différentes zones géomorphologiques du récif de Salary, à Madagascar. Nous avons également examiné les données de hauteur de marée modélisées sur la période de déploiement ainsi que sur un cycle tidal de 18,6 ans.
4. Les enregistreurs subtidaux ont montré des températures moyennes similaires, mais jusqu'à 27% de différence dans les heures cumulées au-dessus de 30 °C. Comparées aux jeux de données de température interpolées, les observations des enregistreurs ont révélé des extrêmes plus élevés et des minima plus bas, soulignant la plus grande fidélité des mesures *in situ*.
5. L'enregistreur intertidal a mis en évidence un stress thermique extrême (jusqu'à 48,8 °C) dans les habitats exploités par la pêche à pied, les événements maximaux de chaleur

survenant durant les saisons de transition plutôt qu'au cœur de l'été austral. Les analyses tidales ont montré que les marées basses de milieu de journée, propres à ces périodes de transition, entraînent un réchauffement intertidal extrême.

6. Les pêcheries de Madagascar connaîtront probablement des risques thermiques inégaux et distincts selon les saisons. Les stratégies d'adaptation au climat doivent donc intégrer la variabilité microclimatique qui module la vulnérabilité socio-écologique des océans côtiers.

Introduction

Chronic warming trends and acute heatwaves, already predicted to accelerate under climate change in the tropical Western Indian Ocean (WIO) (McClanahan et al. 2009; Harrington and Otto 2020; Mawren et al. 2022; Thoral et al. 2022), are predicted to increase temperature trends within reef systems. Due to complex interactions between bathymetry and water movements in the near-shore zone of coastal reefs, distinct microclimates may arise and experience climate change differently from the open ocean. Since human activity is greatly concentrated in these coastal zones, understanding the current and future microclimatic trends of reefs can greatly improve conservation and management decision-making (Woodson et al. 2019). Coastal socioeconomic systems in the WIO are strongly linked to the ecological functioning of ecosystems, and are thus predicted to be at a higher risk of disruption compared to areas of more rapid warming in developed countries (Cinner et al. 2012; Le Manach et al. 2012; Cullen-Unsworth et al. 2014).

Within the WIO, southwestern Madagascar is a region particularly vulnerable to the social and ecological impacts of climate change and heatwaves. Reefs in the region provide critical fisheries and ecosystem services for people in nearby cities and villages, where livelihoods and income are highly dependent on the reef function in proportion to the rest of the WIO (Allison et al. 2009; Harris et al. 2010; Cinner et al. 2012; Gough et al. 2020; Ranaivomanana et al. 2023). However, compound stressors from climate change, elevated fishery pressure, decreasing water quality, enhanced cyclone activity, changing land use patterns, and increasing populations due to coastal migration have placed profound stress on these reefs (Bruggemann et al. 2012; Andréfouët et al. 2013; Carter et al. 2022). While much of the conservation focus on the fringing reef system of southwestern Madagascar has been on unsustainable harvest and adherence to marine protected area (MPA) policies, there has been relatively little work

examining the sensitivity of this marine system to climate change. Nonetheless, these reefs are critically imperiled by thermal stress (Ateweberhan and McClanahan 2010; D'Agata and Maina 2022; Obura et al. 2022), which contributed to historic wide-scale coral bleaching in the region in 1998 and 2016 (Obura et al. 2022; Randrianarivo et al. 2022).

However, assessments of seawater temperature on reefs in southwestern Madagascar have almost exclusively been made using remote-sensed data products (McClanahan et al. 2009; Harris et al. 2010), which masks the information from coastal reef ecosystems in which most artisanal fisheries operate. Internal waves, water mass pooling, and other hydrodynamic phenomena can result in subtidal heterogeneity on reef systems, further complicating assessments of thermal stress on complex coastal reef systems (Leichter et al. 2005; Davis et al. 2011; Woodson et al. 2019; Reid et al. 2020; Brown et al. 2022). Reef flat and shallow lagoon environments are expected to experience higher average and maximum temperatures than deep lagoons and backreefs/forereefs, mainly due to the mixing of cooler offshore waters from greater depths with warmed shallow waters (Reid et al. 2020; Kekuewa et al. 2021; Brown et al. 2022). Therefore, fisheries that are spatially segregated across depth and distance offshore may end up fishing in different thermal microclimates.

In addition to national and multinational industrial fishing, a large proportion of fisheries in the WIO are artisanal (catches sold at the market) and subsistence (catches consumed at home), and provide much of the coastal population's nutrition and livelihoods (Le Manach et al. 2012; White et al. 2022). In the WIO, men and women tend to fish in different habitats using distinct gear, with men typically using boats to access offshore sites and employing nets and lines, but also fishing on foot. Women, by contrast, fish on foot in nearshore areas, harvesting benthic invertebrates with hand-held tools (Westerman and Benbow 2013; Fröcklin et al. 2014; Baker-Médard and Kroger 2024). This type of fishing by foot, or gleaning, is the predominant fishing method for women and low-income households (Cinner and Bodin 2010; Fröcklin et al.

2014)Fortuna-Jackson *forthcoming*(Cinner and Bodin 2010; Fröcklin et al. 2014). Gleaning, (fishing on foot) tends to be restricted to coastal areas accessible by foot, such as mangroves, intertidal flats, seagrass beds, and reef crests, and occurs primarily during calmer seasons (de la Torre-Castro et al. 2017; Lemahieu et al. 2018; Grantham et al. 2021; Tilley et al. 2021; Wallner-Hahn et al. 2022). While men engage primarily in boat-based fishing, some—often those with fewer economic resources—practice gleaning, which does not require a boat or substantial capital investment. Similar species can be found in both deep and shallow habitats, the species composition and abundance within catches vary dramatically between habitats (Fröcklin et al. 2014; Jankowski et al. 2015; Medina-Valmaseda et al. 2020; Stiepani et al. 2023).

Given the asymmetric impact of climate change and heatwaves (marine and atmospheric) on shallow water coastal ecosystems, it is possible that species and populations targeted by women and the least wealthy of a given fishing community will be impacted first and to a greater magnitude than fisheries dominated by slightly wealthier men in deeper waters. This is especially significant given the importance of gleaned organisms for nutrients in the local food supply. Further, it's likely that pressure will increase on gleaning fisheries with climate change, drought, and overfishing, which are transitions from boat-based fisheries and inland agriculture to gleaning (Willer et al. 2023).

Complicating any assessment of thermal stress on this reef system is the additional interaction of the macrotidal semidiurnal tide system in southwestern Madagascar, with a tidal range of around three meters (Chevalier et al. 2015; Moustapha et al. 2021). These tides expose reef flats and even the reef crest at periodic intervals, providing opportunities for gleaning to occur. Tidal emersion on reefs, when timed with solar exposure, can result in devastating bleaching in corals and mass mortality in reef invertebrates, including lucrative fished species such as sea cucumbers (Glynn 1968; Yamaguchi 1975; Anthony and Kerswell

2007; Buckee et al. 2020, 2022; Mejía-Rentería et al. 2020; Schoepf et al. 2020). Given the additional factors of tidal cycles, reef hydrodynamics, and substrate albedo, satellite-derived temperature measurements are inappropriate to describe the thermal environment in which both reefs and fisheries coexist in southwestern Madagascar.

Analyses of climate sensitivity of Malagasy reefs and fisheries have historically been limited to satellite-derived sea surface temperature products, potentially ignoring microclimatic complexities on reefs that experience a spatial segregation of fishery types. Here, we describe the thermal environment of Salary Reef, southwestern Madagascar, across three reef geomorphic zones (backreef, lagoon, and flat) that encompass subtidal and intertidal sites by deploying long-term temperature loggers. We hypothesize maximum temperatures and variability to be highest at intertidal reef flat sites, and amongst subtidal sites, to be highest in backreef and shallow lagoon environments. These zones encompass fishing sites regularly used separately by boat-based and gleaning fishers, thereby describing the thermal environment used by fisheries-targeted species. We further modeled the 18-year tidal cycle (Denny and Paine 1998) of Salary Reef to assess reef flat immersion timing on a yearly, seasonal, and daily basis.

Methods

Study Site

The study was conducted on Salary Reef (22.53 S, 43.25 E; Figure 2), a fringing reef system located in southwestern Madagascar, approximately 100 km north of the region's major city, Toliara. This fringing reef system is part of "Mikea Coast", and is distinct from the major, better-studied barrier reef off the coast of Toliara, Grand Récif de Toliara (GRT), because it receives little riverine inputs. The GRT has long been known to be influenced by the hydrology

of the Onilahy and Fiherenana rivers, and excess sedimentation from upstream terrestrial activities such as mining and agriculture has partially contributed to the decline of the GRT (Pichon 1978; Andréfouët et al. 2013). However, Salary Reef is relatively uncoupled from terrestrial activity and is in better ecological condition than the GRT. This fringing reef system is composed of intertidal flats sloping to a sandy-bottomed lagoon varying 2-5 km in width (~5-15 m depth). The reef crest is periodically emersed during low-tide events, and complex reefs dominate the far reef slope (Randrianarivo et al. 2022, 2023). Further, southwestern Madagascar can be considered a meso- to macrotidal system – tidal ranges can extend up to 5.5 meters (near Besalampy), exposing extensive reef flats and parts of the barrier/fringing reef crest. The Soariake MPA, managed by the Soariake Association with technical assistance from the Wildlife Conservation Society (WCS), was formally protected in 2015 to balance conservation and fishing and encompasses all of Salary Reef and the northern portion of the fringing reef system, but adherence by small-scale artisanal fishers is variable (Zafimahatradraibe et al. 2025). Most boat-based fishing activity occurs on the forereef and in the lagoon, while gleaning can occur both in the shore-adjacent reef flat and on the reef crest itself.

Logger Deployment and Recovery

We deployed ten temperature loggers (ElectricBlue T7.3, Porto, Portugal — all IDs SALEB# “Salary ElectricBlue”) between July 28th and August 10th, 2023, distributed between four reef geomorphic zones (reef flat, lagoon, backreef, and forereef) between 2-4 m depth (Figure 1, Figure 2, Supplemental Table 2). We classified reef flat locations as representative of intertidal gleaning sites, as we were not able to deploy loggers directly on the reef crest. Lagoon, backreef, and forereef sites represented boat fishing locations. Additionally, we selected a site at the Salary Bay dive center to measure the air temperature at 2 m above ground. For all but the air temperature logger, we did not attempt to shade loggers from solar

radiative warming (Bahr et al. 2016; Colin and Johnston 2020; Rich et al. 2024), so as to replicate the microclimate or body temperature that may actually be experienced by exposed sessile marine organisms in each geomorphic reef zone (Kearney 2006; Jimenez et al. 2008; De Frenne et al. 2025). Temperature data should therefore not be interpreted as seawater temperature, but as a record of potential benthic ectotherm body temperature. The simple use of seawater (or air) temperature to understand potentially stressful periods fails to account for the complexities of an organism's heat budget, even in submerged environments.

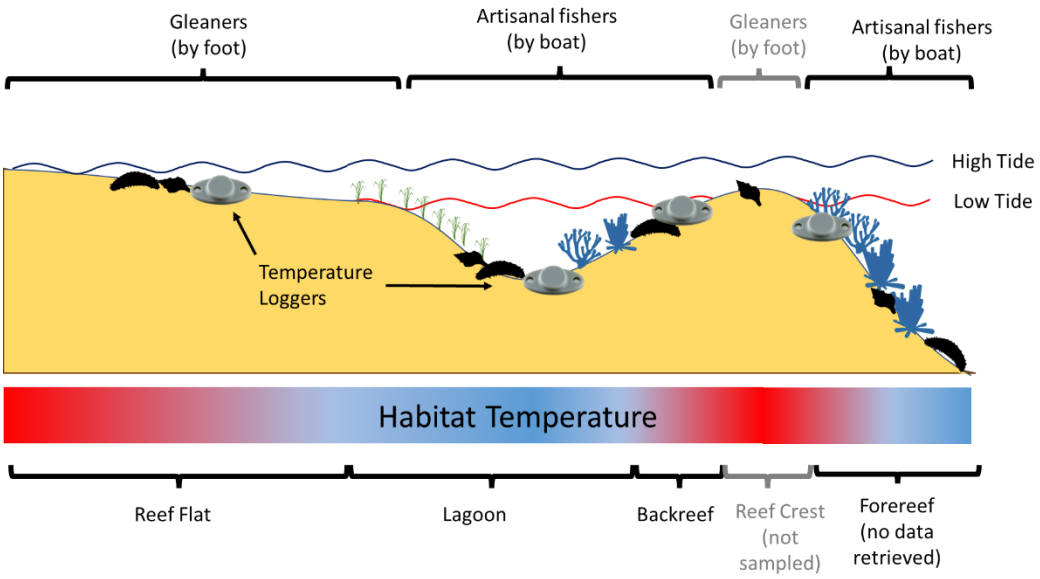

Fig. 1 A cross section of a typical reef system of southwestern Madagascar with corresponding fishing zones and logger deployment locations is shown. The reef flat and reef crest (not sampled) are the intertidal portions of these reef systems, on which gleaning occurs during low tide events. The reef lagoon, backreef, and forereef are subtidal zones that are mainly fished by boat.

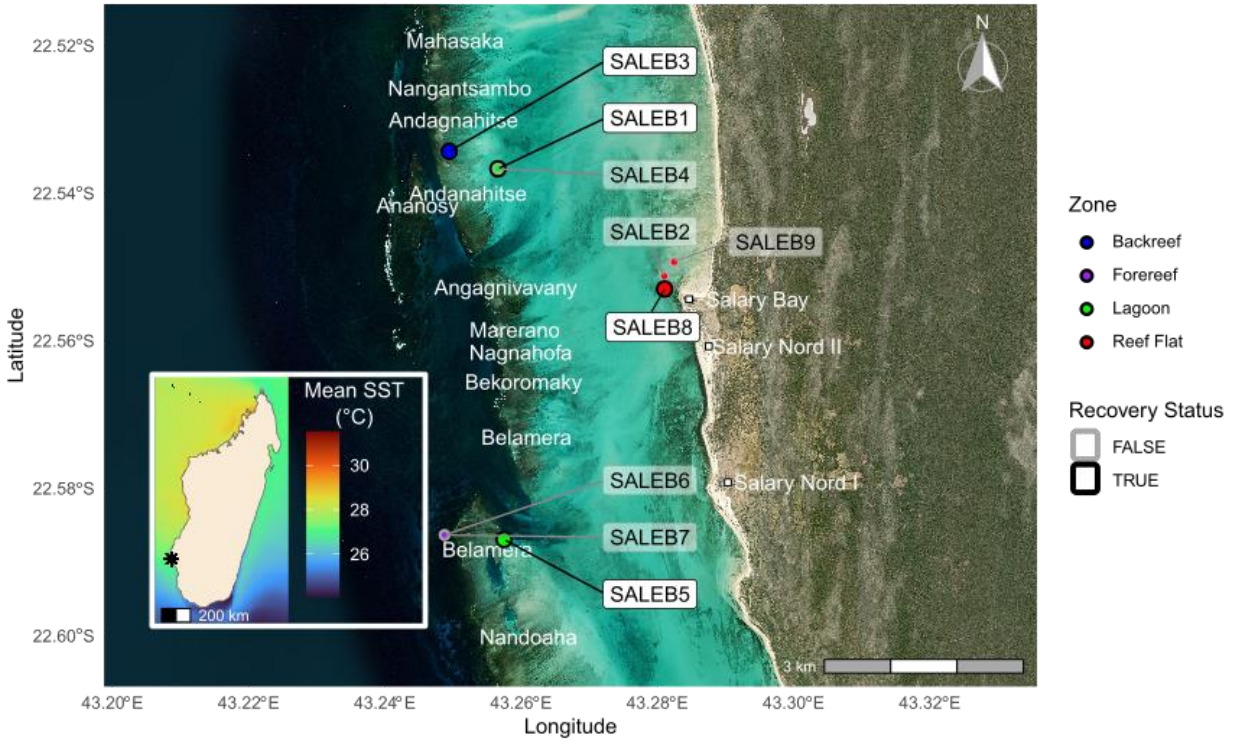

213

214 **Fig. 2** Logger deployment sites near the village of Salary in southwestern Madagascar are
215 shown. Large colored points show recovered logger locations with their corresponding reef
216 geomorphic zone. Unrecovered loggers are shown outlined in gray. Of the nine deployed
217 loggers on the reef, we recovered four loggers across three of the reef's geomorphic zones. The
218 locations of fishing sites are indicated with labels, while the location of the air temperature
219 logger is not shown. The inset map depicts the location of Salary Reef within Madagascar with
220 accompanying mean yearly sea surface temperatures (2002-2009, Bio-ORACLE, (Assis et al.
221 2024).

222 We affixed loggers to the reef using UV-resistant zip-ties and Splash-Zone two-part

223 marine epoxy (Modern Recreational Technologies, Hickory, NC, USA). We selected crevices for

logger deployment to reduce breakage from wave action and record temperatures of these reef refugia for many targeted fishery species. We recorded GPS coordinates with up to 5 m accuracy (Garmin eTrex 10) and recorded videos of logger placement (GoPro Hero8 Black) to facilitate recovery. Temperature logger accuracy was set to 0.1 ºC, recording every 15 minutes. We recovered five loggers after at least one year (Supplemental Table 2). Logger deployment and recovery were accomplished by freediving.

Data Analysis

Temperature Data

Of the ten temperature loggers deployed, we recovered five (four reef loggers, one air temperature logger) after at least 357 days (SALEB8, Flats) and at most after 459 days (SALEB1). Although some loggers collected data for over a year, we focused our comparative site analysis on only the dates where all four recovered water temperature loggers actively collected data (357 days).

To compare our logger-recorded reef temperatures against commonly used remote-sensed products, we further downloaded and extracted seawater temperature data from NOAA OISST (Optimal Interpolated Sea Surface Temperature; (Huang et al. 2021) and Copernicus Global Physics Analysis (European Union-Copernicus Marine Service 2016) at -22.6° S, 43.25° E. OISST records sea surface temperatures were available at 1/4° resolution, while we selected Copernicus temperature records from a depth of 0.5 m at a 1/12° resolution. We calibrated our air temperature data against downscaled ERA5 models of air temperature using the *mcera5* R package (Klinges et al. 2022).

Tidal Regime

As no tide stations are available in southwestern Madagascar, we used the package *pyTMD* (Sutterley et al. 2024) in Python (v. 3.10.15) to calculate tide heights at the coordinates -22.6° S, 43.25° E between the years 2006-2024. This timescale was chosen to encapsulate the 18.6-year lunar cycle to which short-term tidal cycles respond (Denny and Paine 1998). It further illustrates whether the tidal regime recorded in our 2023-2024 intertidal temperature data represents the long-term trend for this location. We used the TPXO9 (v5, 1/30º resolution) atlas model of global tides constituents (Egbert and Erofeeva 2002). For some of our analysis, we grouped tide data by four seasons — early hot-wet (November-January), late hot-wet (February-April), early warm-dry (May-July), and late warm-dry (August-October). Initial exploration of the intertidal logger data indicated that distinct temperature regimes occurred along the four seasonal divisions listed above, and so, we processed some of our tidal data using this seasonality.

We used a custom script to determine the relative tide height and tidal exposure regime of the intertidal temperature logger (SALEB8 Flat), based on significant temperature “drops” correlated with rapid cooling or warming of temperature loggers when exposed to air or water (Harley and Helmuth 2003; Gilman et al. 2006). We determined the intertidal temperature logger to have a height of -0.956 m (relative to average height) and +22 minutes behind the modeled tide series obtained via the *pyTMD* package. From this tide height, we reconstructed the immersion status of each time point from the intertidal temperature logger time series. When determining the decadal patterns of low-tide exposure, we used the rounded height of this logger (-1 m, relative average modeled height) as a threshold beyond which we calculated hours of exposure.

Statistical Analysis

All statistical analysis was completed in R (v. 4.2.1). For cross-site comparisons, we filtered available water temperature datasets to only the dates that data had for all sites (July 29th, 2023, to July 20th, 2024). We used a Kruskal-Wallis non-parametric test to determine if median site temperatures were different, and then *post hoc* Bonferroni-adjusted Dunn's test package to determine pairwise site significance.

We used wavelet analysis to determine the temporal patterns in power spectra during the deployment period of our temperature data time series. By decomposing temperature periodicity on a time basis, this method allows for the detection of non-stationary periodicity in environmental time series and provides an advantage over traditional power spectra analysis (Rivest and Gouhier 2015). We used the *WaveletComp* package to decompose and visualize the wavelet spectra using default Morlet wavelets (Roesch and Schmidbauer 2018).

Results

Reef Microclimate Variability

Of the three subtidal data loggers (SALEB1, SALEB3, and SALEB5), the backreef site (SALEB3) had the highest overall mean (27.3 ºC) and maximum (33.4 ºC) temperatures (Figure 3). It also spent a similar number of hours above the Coral Reef Watch (CRW) bleaching threshold of 30 ºC (Southwestern Madagascar Coral Reef Watch threshold, (Skirving et al. 2020) as the shallow lagoon site (SALEB1, Supplemental Table 1). The deep lagoon site (SALEB5), the deepest one overall, had the lowest mean (27.08 ºC) and maximum temperatures (33.0 ºC), and the fewest number of hours (1089.2 h) above the CRW 30 ºC threshold. A Kruskal-Wallis test confirmed that water temperature was significantly different between sites ($H_2 = 160.5$, $P < 0.0001$). *Post-hoc* multiple comparisons indicated significant

differences between all sites, although the significance between the two shallow sites was weak (SALEB1 x SALEB3, Bonferroni-adjusted multiple comparison, $P = 0.0452$), while the deep lagoon site SALEB5 was significantly cooler than both shallower sites (Bonferroni-adjusted multiple comparison, $P < 0.0001$).

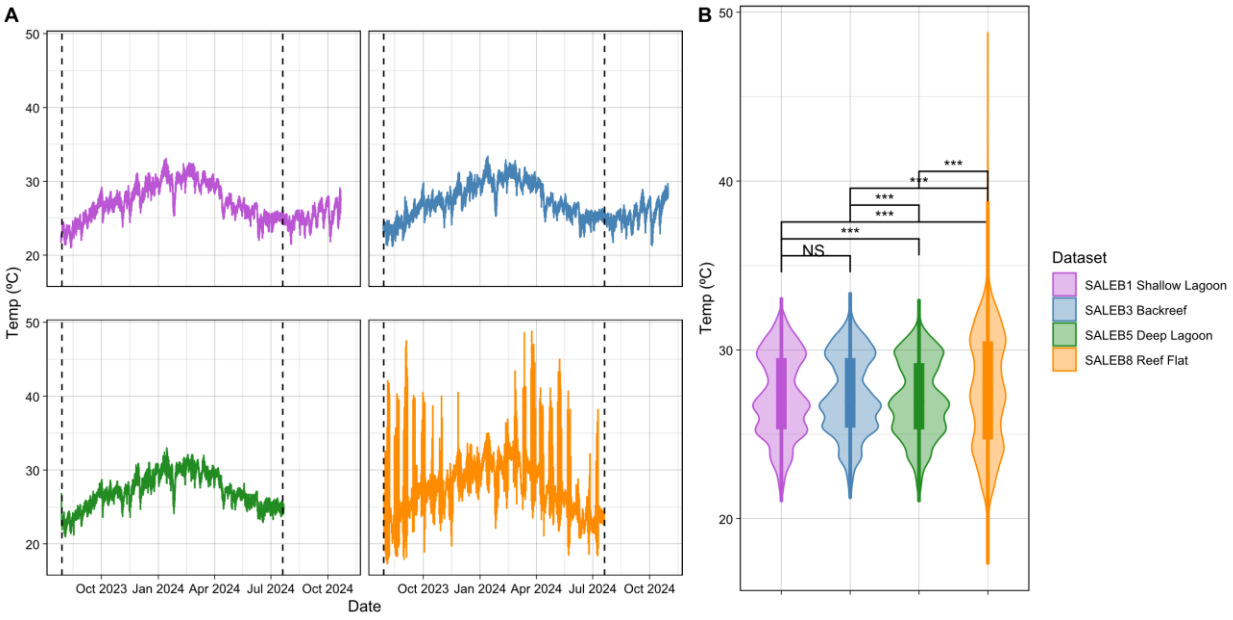

Fig. 3 A Temperature time series from the four recovered loggers on Salary Reef, SW Madagascar, are shown. Vertical dashed lines indicate the extent of data used for site comparisons. Data were collected every 15 minutes. **B** The distribution of temperatures at each site is shown. Boxplots indicate mean and interquartile range (25-75%). Asterisks give multiple comparisons (Wilcox's) significance across all loggers – note that in the text, we restrict our multiple comparisons to just subtidal sites, and therefore, there are slight differences in significance level.

We further calculated the daily variance and temperature range of each subtidal logger, and only the temperature range was significantly different between sites (Daily Variance Kruskal-Wallis, $H_2 = 3.69$, $P = 4.72$; Daily Range Kruskal-Wallis, $H_2 = 16.7$, $P = 0.0002$). The daily temperature range was highest at the backreef site SALEB3 and lowest at the shallow lagoon site SALEB1 (Table 1). Post-hoc comparisons demonstrated that the temperature range at the backreef site was only significantly different from the shallow lagoon site (SALEB1 x SALEB3, Bonferroni-adjusted multiple comparisons, $P = 0.000135$). Despite having a mean

temperature of only 0.18/0.21 °C below and a maximum temperature only 0.1/0.4 °C the shallow lagoon and backreef sites respectively, the deep lagoon site had 27% fewer hours above 30 °C compared to these sites.

Table 1 A Summary statistics of temperatures recorded on Salary Reef, calculated between 2023-07-29 and 2024-07-20, and reanalysis products used to compare the accuracy of *in-situ* loggers against commonly used sea surface temperature data sources. **B** To compare our *in-situ* data against the daily reanalysis temperature timeseries, we performed a daily summarization of subtidal logger data. Additional details about *in situ* loggers can be found in Table S2. *Denotes maximum air temperature values that were not calculated due to a short period of logger exposure to direct sunlight

A) Data Source	ID	Zone	Mean (ºC) ∓ SD	Minimum (ºC)	Maximum (ºC)	Hours Above 30 ºC	Daily Range (°C) ∓ SD
In-situ logger	SALEB1	Shallow Lagoon	27.26 ∓2.43	21.0	33.1	1478	1.49 ∓ 0.48
In-situ logger	SALEB3	Backreef	27.29 ∓2.33	21.2	33.4	1446	1.7 ∓ 0.63
In-situ logger	SALEB5	Deep Lagoon	27.08 ∓2.26	21.0	33.0	1089	1.58 ∓ 0.57
In-situ logger	SALEB8	Reef Flat	27.64 ∓3.57	17.3	48.8	2510	6.42 ∓ 6.42
In-situ logger	SALEB10	Air Temperature	26.36 ∓ 4.6	12.3	*	1917	11.45 ∓ 2.81

B) Data Source	ID	Zone	Mean (ºC)	Minimum (ºC)	Maximum (ºC)	Days Above 30 ºC
Reanalysis	Copernicus Global Ocean Physics Analysis and Forecast		27.34 ∓ 2.44	22.91	31.96	15.75
Reanalysis	NOAA/NCEI OISST V2		27.22 ∓ 2.07	23.05	30.66	9
Daily summarized in-situ logger	SALEB1	Shallow Lagoon	27.27 ∓ 2.39	21.70	31.82	14

Daily summarized in-situ logger	SALEB3	Backreef	27.3 ∓ 2.3	21.94	31.59	13.5
Daily summarized in-situ logger	SALEB5	Deep Lagoon	27.09 ∓ 2.21	21.84	31.32	10.75

The seawater temperatures measured *in situ* summarized as daily means and those measured from reanalysis products (OISST, Copernicus) were not significantly different, indicating that variability driving site-level differences occurs on a sub-daily timescale (Kruskal-Wallis test, $H_2 = 4.722$, $P = 0.0943$, supplemental Fig. 1). Correlation ranged between 0.86 – 0.96 (R^2, SALEB8 Reef Flat – SALEB3 Shallow Lagoon) for water logger data and Copernicus data, and between 0.76 – 0.92 (R^2, SALEB8 Reef Flat – SALEB5 Deep Lagoon) for logger data and OISST data (supplemental Fig. 3). However, OISST tended to underpredict the hottest values observed with loggers, while the Copernicus dataset at a 0.5 m depth better matched the distribution of observed data (Table 1, supplemental Fig. 1). Correlations between each 15-minute logger observation and daily reanalysis data were lower than the summarized logger data values, with correlations ranging from 0.62 – 0.93 (R^2, SALEB8 Reef Flat – SALEB1 Backreef) for water logger data and Copernicus data, and between 0.54 – 0.89 (R^2, SALEB8 Reef Flat – SALEB5 Deep Lagoon) for water logger data and OISST data (supplemental Fig. 4).

The intertidal temperatures collected at SALEB8 (Reef Flat) were radically different from the other subtidal temperature series due to periods of air exposure during low tide. Both exposure during low tide and the day/night cycles modulated the temperatures experienced at this site, indicated by strong wavelet power levels associated with 8-hour (length of submersion), 12.4-hour (diel tidal cycle), and 24-hour (daily cycle) cycle periods (Figure 5). Vertical bands below the 12.4-hour periods correspond to a combination of tidal harmonics and variable emersion durations under seasonally changing tidal amplification. Average emersion duration was 2.36 hours (median 2.47 hours), although the left-skew of tidal emersion duration indicates longer durations, up to 3.7 hours, are more frequent (supplemental Fig. 7). The three

other subtidal loggers showed power bands over the 12.4- and 24-hour wavelet periods, again indicating the influence of tidal and solar cycles on temperature regimes on the subtidal reef (supplemental Fig. 8). Finally, the air temperature recorded by the temperature logger displayed an obviously strong 24-hour wavelet period power band, corresponding with solar cycles, but also a seasonally moderate 12-hour power band corresponding to atmospheric tides and land-sea breezes that are stronger during the cloudless warm-dry season (supplemental Fig. 8).

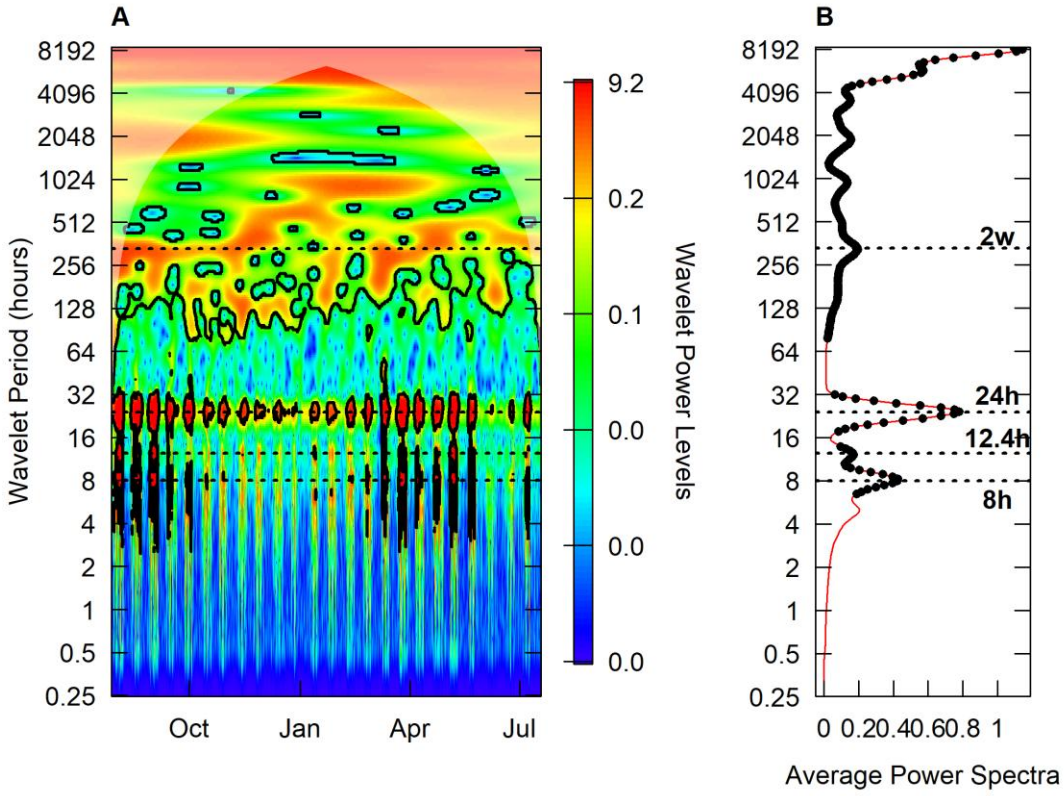

Fig. 5 A Wavelet analysis of intertidal reef flat (SALEB8) temperature between August 2023 and July 2024. Black outlined areas indicate regions that have strong wavelet power support ($p < 0.01$). **B** Average power spectra illustrate the strongest periods observed over the logger deployment period. Black dots correspond to periods that were strongly statistically significant ($p > 0.01$). Across both plots, four power ridges centered around 8 hours, 12.4 hours, 24 hours, and 2 weeks correspond to tidal exposure, tidal cycle, daily solar cycles, and tidal flushing/upwelling events, respectively. Periods of ~8 hours correspond to the longest tide cycles that exposed the logger for the longest, and the decreasing power of vertical bands indicates the gradually shorter tide cycles that exposed the logger for less and less time. High

power levels between the 128h and 1024h wavelet periods (encompassing a 2-week significant band) may correspond with tidal flushing of the lagoon (Chevalier et al. 2015).

The intertidal temperature data showed a strong seasonal pattern; we recorded extreme temperatures not in the peak wet season/January, but between March to June, and August to October. Loggers recorded a maximum temperature of 48.8 °C on March 24th, 2024, with additional excessive heat days occurring on March 12th, 2024 (48.6 °C) and September 3rd, 2024 (47.5 °C). Between November and February, water temperatures were consistently warmer than the air temperature in the intertidal zone, despite this being the hottest portion of the year in southwest Madagascar. These extreme temperatures can be attributed to low-tide events (Figure 4A). Examining the residuals of the relationship between the intertidal (SALEB8) and lagoon (SALEB5) loggers (linear model, $R^2 = 0.64$, $P < 0.0001$) reveals minimal variation from zero residuals in submerged observations (Figure 4B). However, exposed observation residuals alternate between much warmer (~5-20 °C, March-October) and cooler (~ -5 °C, November-February) than the water temperature in the lagoon. In short, low-tide temperatures were lower than other parts of the year, and indeed lower than water temperature, during the hottest part of the year (wet season, November-March). Water temperature residuals were not significantly different between night and day observations (Figure 4C).

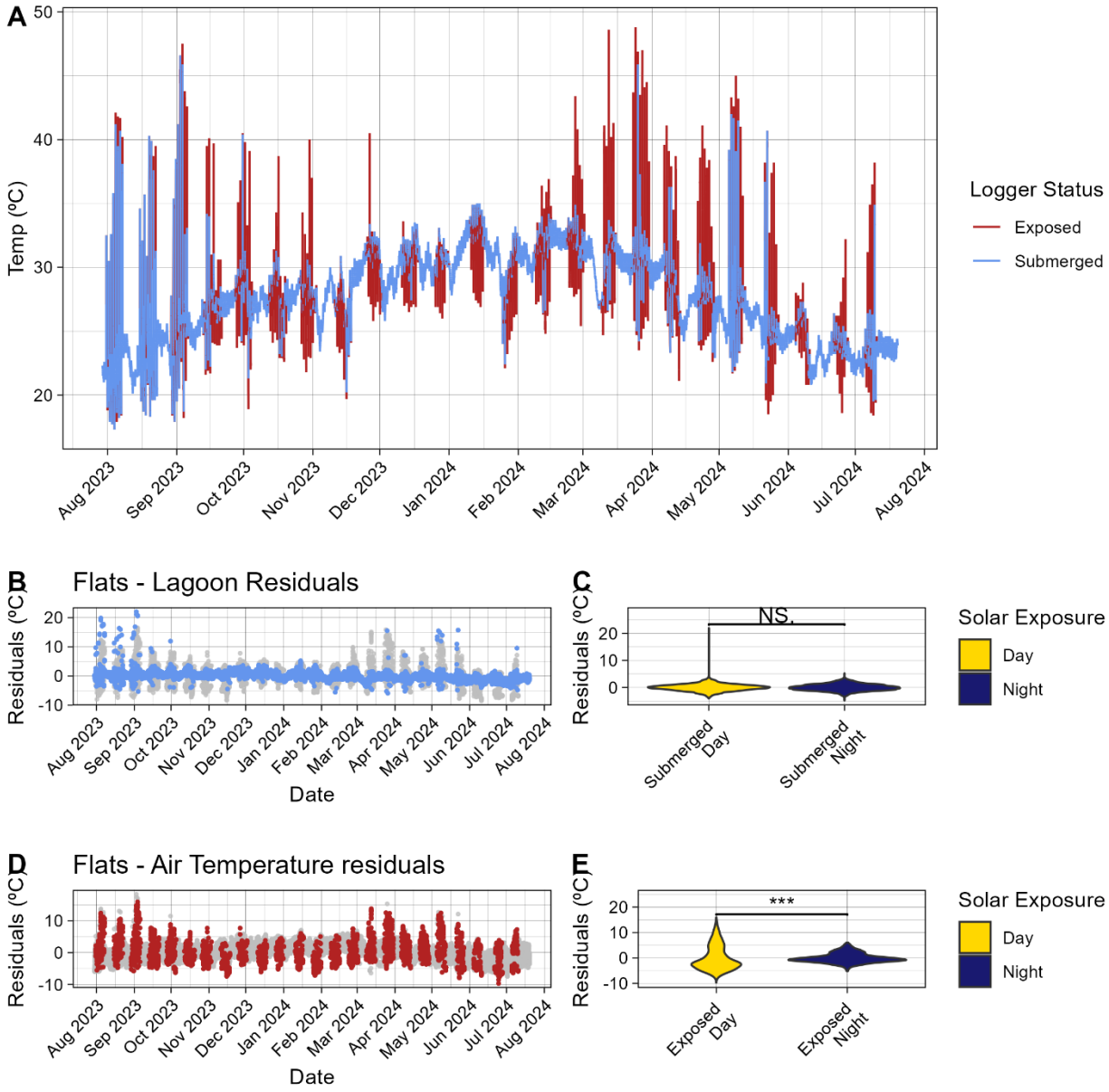

Fig. 4 A Tidal exposure status of the intertidal flat (SALEB8) logger. Air exposure/water submersion status was determined via the application of interpolated logger tide height and offset from tidal model predictions. Logger status predictions in August and September 2023erroneously identified heat spikes more often associated with low tide as submergence events. Temperature residuals from the lagoon (**B-C**, SALEB5) and air temperature residuals (**D-E**, SALEB10) from intertidal zone temperatures (SALEB8) are also shown. In **B**, nonzero residuals of submerged observations indicate differences in water temperature at the intertidal site. These submerged residuals were not different between day and night observations (**C**). When examining residuals of exposed observations in **D**, nonzero observations indicate times when the exposed intertidal logger was warmer or cooler than the air temperature at Salary. Residuals of exposed observations were significantly different between day and night exposures (**E**).

Residuals of the relationship between observations of the intertidal logger (SALEB8) and the air temperature (SALEB10) (linear model, $R^2 = 0.44$, $P < 0.0001$) show that low-tide logger temperatures were much warmer than air temperature, indicating the importance of additional microclimate factors (e.g., albedo, radiative forcing) on low-tide temperature on intertidal flats (Figure 4D). During the hot, wet season, the intertidal flat logger experienced fewer positive residual spikes with low tide while periodically having negative residuals. However, during the warm, dry season, flat logger temperatures routinely exceed air temperatures. The most extreme negative residuals were recorded during the daytime (Figure 4E). Mean hourly air temperatures recorded using temperature loggers generally matched those from ERA5 microclimate downscaling data ($R^2 = 0.84$, supplemental Fig. 2)

Decadal Tide Patterns

Tides during the field season of 2023-2024 occurred during a weakening in the 18.6-year lunar cycle — low tides were less extreme than at the peak of the cycle in 2015-2016, particularly in the early warm-dry (May-Jul) and early hot-wet seasons (Nov-Jan; Figure 6, supplemental Fig. 5). The maximum tidal range near the Salary reef was 3.4 m. However, through additional data exploration, we found that the tidal range increased to over 5.5 m moving northward to a point off the northwestern coast of the Besalampy district (-16.65 S, 44.42 E)m. However, early warm-dry low tides spend more time below -1 m and have lower overall tides during the day than the night, while the inverse is true during early hot-wet low tides, where nighttime low tides are generally longer and larger. In the late hot-wet and warm-dry months, there is no trend in monthly hours below -1 m or monthly minimum tide across years, indicating that the timing of extreme low tides is consistent along the 18.6-year tidal cycle. Tidal heights that exceed -1 m (and would therefore expose the intertidal flats logger) routinely occur between 09:00 and 15:00 (EAT) across the 18.6-year tidal cycle, encapsulating

solar noon (supplemental Fig. 6). Low tides that expose reef flats below a -1 m elevation are therefore consistent in their diel and annual timings, although interannual extremity varies.

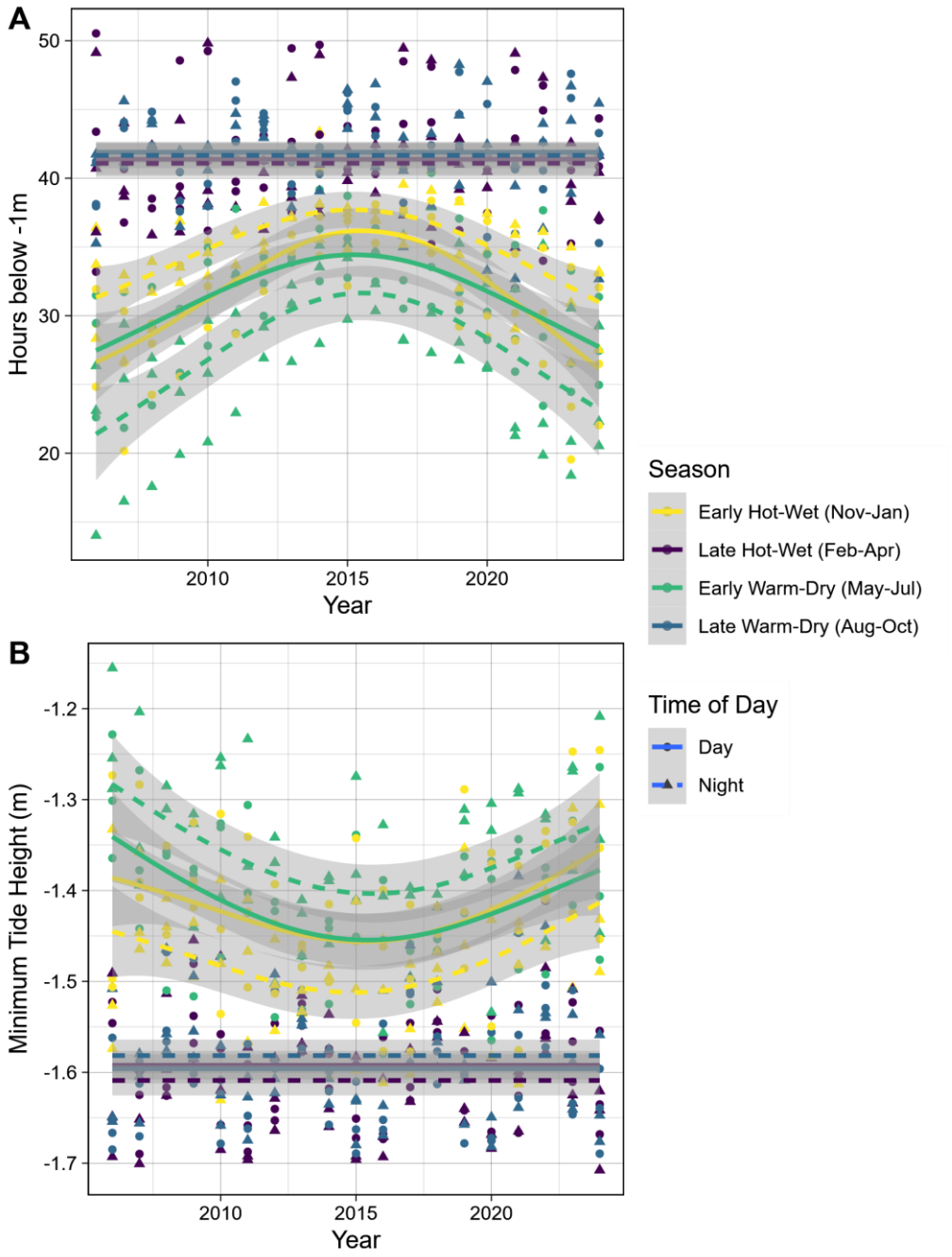

Fig. 6 A Hours spent below –1 m (mean tide, TPXO9 tide model) and **B** minimum tide height (TPXO9 tide model) for each month at Salary Reef between 2006 and 2024 (18 years) across austral seasons (Hot-Wet = November-April, Warm-Dry = May-October) and daily sun cycles. Lines of fit are loess lines. Each point represents the monthly maximum hours below –1 m or

minimum tide height (split by day and night), so that there are 24 data points each year (12 monthly calculations across day and night cycles).

Discussion

Through our analysis of *in-situ* temperature data and long-term tidal amplification, we uncovered heterogeneity and extremity across three geomorphic zones within a barrier reef system in southwestern Madagascar. Subtidal sites, while having superficially similar thermal regimes, exhibited up to 27% more heating hours (hours above 30 °C, deep vs. shallow lagoon). Such variance and variation in extremes across temperature series with similar means is common when comparing time series from loggers deployed on reef flats/back reefs and deeper reef sites (Guadayol et al. 2014; Cyronak et al. 2020). However, due to the relatively large tidal range and depth of the lagoon (~15 m max), we see less fine-scale variation in subtidal station temperatures than typical coastal lagoons in microtidal settings (Pichon 1978). Many of the extreme observations across sites (both maxima and minima) were larger than those obtained from two remote-sensed products, indicating that *in-situ* logger observations describe the thermal environment with more fidelity. This is a common observation, as remote-sensed and reanalysis products often mask coastal areas, spatially average, and do not account for other microclimatic processes such as substrate albedo and water residence time (Castillo and Lima 2010; Bos and Pinsky 2025; Margaritis et al. 2025; Thompson et al. 2025). Interestingly, the subtidal sites at Salary Reef all had larger temperature maxima (February 2020: 30.7 °C, depth = 25m, February 1964: 30.25 °C, depth = 10m) and minima (April 2020: 21.5 °C, depth = 25m, July 1964 21.45 °C, depth = 10m) than reported from the nearby GRT (Pichon 1978; Godefroid et al. 2024). Variation between January and May at the GRT was much higher than at other times of the year at the same site, including the (on average) cooler months of July and August. This was attributed to the influence of larger tides (observed in our study), increased cyclone activity, and internal waves arising from increased wind activity during this period (Farquhar et

al. 2022; Godefroid et al. 2024; Thompson et al. 2025). Overall, diel heat flux across the reef can be attributed to daytime solar irradiance, which is modulated by the interaction of atmospheric (cloud cover, wind speed, solar azimuth) and oceanic (tidal range, depth, wave height) conditions (Davis et al. 2011; Zhang et al. 2013; Cyronak et al. 2020).

While all subtidal loggers indicated an expected trend pattern of elevated temperature exposure during the hot-wet season (January-February), temperatures recorded from the intertidal flat logger displayed a contrasting pattern of elevated temperatures during the shoulder seasons. Our wavelet analysis of this intertidal logger confirmed a weakening of 24-, 12.4-, and 8-hour bands during the hot-wet season, which is explained by the decreased tide amplification during this period. Further, the lack of warming compared to ambient air temperature in the hot, wet season suggests sufficiently low tides did not occur during the daytime. The relative cooling of logger temperatures throughout the year further indicates convective cooling from wind can reduce thermal exposure below ambient air temperatures, even during the day (Helmuth et al. 2011). However, data from 1961 indicated temperatures of 41 °C in pooled water on the exposed reef crest of the GRT between November and December. Interestingly, this observation timeframe corresponds with the annual minimum tidal amplitude we describe on nearby Salary Reef (Pichon 1978) where we did not observe intertidal temperatures in excess of 38 °C. The maximum decadal tidal amplitude occurred in 1959, and so we can contextualize the 1961 extreme temperatures in this same season as the product of shorter low-tide durations and heights in the present day than in 1961. It is therefore possible that even more extreme temperatures would have been recorded in 1961 if data were recorded during the annual maximum tidal amplitudes of November-January or May-July. Indeed, we quote directly from Pichon (1978):

467 "*The data we have are actually too fragmented to permit an exact appreciation of the*
468 *importance of this warming phenomenon of waters on the reef flat.*" [1]

469 Our long-term analysis of the tide series over an 18.6-year cycle indicates that the diel and
470 seasonal timing of longer intertidal exposures are consistent across years, while the length of
471 emersion durations changed year over year. Our data was collected during a relatively low-
472 exposure period of the 18.6-year cycle, suggesting that intertidal logger observations in 2015 or
473 2033 would show hotter, lower, and longer intertidal periods.

474 Bolstered by chronic warming and acute heatwave events, we predict that the next ~16
475 years will see intertidal habitats in southwestern Madagascar experiencing hotter conditions
476 than we observed during our deployment period. This is critical because the two lowest tide
477 windows between February to April and August to October are the most optimal for gleaning,
478 both from a consideration of access to low tidal elevation seafloor and because of the relatively
479 calm seas in this period (Grantham et al. 2021; Farquhar et al. 2022; Maka et al. 2022).
480 Between these tide windows in the warm-dry season, however, wind speeds off southwestern
481 Madagascar increase, which limits the number of days fishermen can access offshore sites and,
482 for gleaners, the exposed offshore reef crest (Pichon 1978; Farquhar et al. 2022). Furthermore,
483 the stationarity of midday low tides throughout the year is a particular risk factor for tropical reefs
484 in southwestern Madagascar. On the Australian Great Barrier Reef, the time forms of the tidal
485 harmonics result in shifting low-tide timing over the year, such that extreme low tides occur only
486 around midday in the winter, potentially offering thermal refuge to intertidal organisms (Buckee
487 et al. 2022).

[1] "*Les données que nous possédons sont actuellement trop fragmentaires pour permettre d'apprécier l'importance exacte de ce phénomène d'échauffement des eaux sur l'ensemble du platier.*"

Inferring Reef Microclimate to Reef Coral and Fishery Resilience

In southwestern Madagascar, gleaning supports a diverse array of species critical to local food security and livelihoods, including sea urchins, bivalves, gastropods, octopus, and fish (Rabesandratana 1985; Herinirina et al. 2023). Among these, sea cucumbers (Bêche-de-Mer, trepang) represent a particularly lucrative commercial resource, harvested alongside more subsistence-oriented species like sea urchin and shellfish. Sea cucumbers, or holothurians, are a relatively abundant target species in protected reef environments and can be found up to the intertidal reef flat zone. Holothurians can be an important part of a gleaner's catch, and additionally, there are major holothurian aquaculture pens in the lagoon of the GRT and numerous other lagoon sites across southwestern Madagascar (McVean et al. 2005; Lavitra et al. 2006; Baker-Médard and Kroger 2024). A majority of holothurians are destined for the export market, and thus can be an important source of currency for gleaners (McVean et al. 2005; Lavitra et al. 2006; Fattebert 2020; Maka et al. 2022). Planktonic larval holothurian densities were the highest between February and April, which correspond with the hottest flat reef temperatures observed (Rasolofonirina and Conand 1998; Lavitra et al. 2006). Further, the highest number of fishers and fishing days occur between April to December, although this seasonality has been attributed to avoiding increased lagoon turbidity due to river flooding in the GRT, which is less of a problem on Salary Reef (Maka et al. 2022).

The underlying coral habitat is also threatened by climate change. Corals and their associated zooxanthellae, Symbiodiniaceae, are able to exhibit moderate tolerance to subtidal heat pulses due to their molecular and cellular plasticity, which can be selected for in highly variable or warm environments (Drury 2020). While some coral colonies exposed to prolonged air exposure during macrotidal regimes have elevated resilience to atmospheric heatwaves (Schoepf et al. 2020; Brown et al. 2024), sufficient heat and air exposure quickly result in intertidal mass mortality across taxa (Glynn 1968, 1976; Schoepf et al. 2015; Ainsworth et al.

2016; Castrillón-Cifuentes et al. 2017; Le Nohaïc et al. 2017; Buckee et al. 2020, 2022; Godefroid et al. 2024). The delineation between resistance/resilience and declines in marine populations is a fine one. Even with local adaptations, *Acropora* coral populations declined dramatically under modeled 3 °C of warming (Lachs et al. 2024). While some might invoke shallow-water/intertidal habitats as a "space-for-time" substitution supporting the potential for organism resilience in a warmer ocean, the fact remains that populations in these reef flat environments are experiencing the warmest temperatures under current conditions, with a hard ceiling of aerial exposure. The hypothetical deadening of shallow-water coastal environments would be devastating for vulnerable gleaning fisheries operating in these marginal environments.

Will intertidal organisms adapt, move, or die in response to an 18.6-year cycle? Previous work investigating intertidal mussels in New Zealand and Washington State, USA, observed a decrease in average mussel intertidal height, a direct product of weakening survival in the upper intertidal and effectively compressing the vertical and horizontal range (Denny and Paine 1998; Sorte et al. 2018). Coupled with rapidly warming air and water temperatures in the WIO region (Ateweberhan and McClanahan 2010; Bruggemann et al. 2012; Lima and Wethey 2012; Harrington and Otto 2020; Obura et al. 2022), hotter low tides may accelerate the depopulation of tidal flat habitats by gleaned species such as holothurians, whelks, and octopi. Over a longer decadal horizon, sea level rise may alleviate heat exposure of tidal flats by increasing inundation hours, at the expense of lost gleaning opportunities during weak low-tide periods (Harborne 2013). Before 1978, extensive coral cover of the reef flat by branching *Acropora* was reported by Pichon from the GRT, approximately 100 km south of Salary. By 2008, this intertidal coral cover was gone, likely due to a mixture of factors including cyclone activity, fishing gear impacts, poor water quality from Toliara, and river discharges (Harris et al. 2010; Andréfouët et al. 2013; Chevalier et al. 2015). Direct attribution of lost coral cover to warming

atmospheric/water temperatures and decadal tidal cycles is therefore not possible with current data, but our data adds context to coral cover declines in southwestern Madagascar.

Conclusions

Whether modeling or managing, the implication of differential seasonal climatic vulnerability in coastal reef and intertidal flats is that a focus on the putative hottest part of the year (hot-wet season, November-April) risks missing the most sensitive season for intertidal habitats. Microclimatic analysis may best describe conditions at a temporal and spatial scale most relevant to coastal human activities, thereby allowing for more careful considerations of the impacts of climate change on people and the ecosystems they rely on. Previous work assessing the climate sensitivity and resiliency of reef fisheries in Madagascar identified the northwest as the most sensitive region to climate impacts due to elevated SST and solar irradiance, but did not consider the importance of tidal regimes or reef microclimates on gleaning fisheries (Cinner et al. 2012, 2022). It should be highlighted that gleaners in the WIO are already well aware of ongoing seawater warming and its negative impacts on their catch, which, coupled with overexploitation, has resulted in reduced mollusk fishery yields (Cochrane et al. 2019; Alati et al. 2020).

As the climate warms, the reef system of southwestern Madagascar will continue to experience more frequent, long, and intense heatwave events amplified by the semidiurnal, mesotidal system. On this reef system, where gender roles, socioeconomic security, and fishery styles are spatially separated, we also uncovered spatial separation in microclimates and ultimately climate sensitivity. Future work could also assess the extent to which socio-ecological systems will be impacted, especially when considering extremes and spatial structure (White and Wulfing 2024; Wulfing and White 2024).

MPAs in Madagascar, including the Soariake MPA within which our study site is located, currently do not account for the impacts of climate change and different fisheries styles. Effective spatial management in coastal reef ecosystems will need to confront different use cases of reef zones that experience different magnitudes and timing of heat stress. In particular, shallow reef areas and the fisheries they support will experience heat stress sooner than deep reef habitats. Therefore, gleaning fisheries will require access to shallow reef zones within MPAs to be managed for their social resiliency. In addition, the promotion of alternative livelihoods to reduce fishing pressure will also be necessary, along with providing a livelihood portfolio in the case of heatwave-induced fishery collapse. By taking a microclimate lens to the thermal landscape of Salary Reef, we advance our spatio-temporal understanding of where extreme heat may be experienced by reef organisms the most, and by extension, the fishers that depend on these reef ecosystems.

Acknowledgements

The authors wish to thank Fred Lucas, Herdinand Haidodiado, and Elizabeth Kroger for the logistical and field support during logger deployment and recovery. Funding to ERW and MBM was provided by NSF grant awards 1923707 and 2409030. Additionally, we would also like to thank Ruscena Wiederholt for their input on earlier versions of this manuscript. Authorization of research was provided by the Direction Générale de la Gouvernance Environnementale of the Republic of Madagascar, n° 357 22 MEDD/SG/DGGE/DAPRNE/SCBE.

Data Availability Statement

Scripts and data will be made available in a public repository upon acceptance for publication.

Citations

Ainsworth TD, Heron SF, Ortiz JC, Mumby PJ, Grech A, Ogawa D, Eakin CM, Leggat W (2016) Climate change disables coral bleaching protection on the Great Barrier Reef. Science 352:338–342

Alati VM, Olunga J, Olendo M, Daudi LN, Osuka K, Odoli C, Tuda P, Nordlund LM (2020) Mollusc shell fisheries in coastal Kenya: Local ecological knowledge reveals overfishing. Ocean & Coastal Management 195:105285

Allison EH, Perry AL, Badjeck M-C, Neil Adger W, Brown K, Conway D, Halls AS, Pilling GM, Reynolds JD, Andrew NL, Dulvy NK (2009) Vulnerability of national economies to the impacts of climate change on fisheries. Fish and Fisheries 10:173–196

Andréfouët S, Guillaume MMM, Delval A, Rasoamanendrika FMA, Blanchot J, Bruggemann JH (2013) Fifty years of changes in reef flat habitats of the Grand Récif of Toliara (SW Madagascar) and the impact of gleaning. Coral Reefs 32:757–768

Anthony KRN, Kerswell AP (2007) Coral mortality following extreme low tides and high solar radiation. Mar Biol 151:1623–1631

Assis J, Fernández Bejarano SJ, Salazar VW, Schepers L, Gouvêa L, Fragkopoulou E, Leclercq F, Vanhoorne B, Tyberghein L, Serrão EA, Verbruggen H, De Clerck O (2024) BIO-ORACLE v3.0. Pushing marine data layers to the CMIP6 Earth System Models of climate change research. Global Ecol Biogeogr 33:e13813

Ateweberhan M, McClanahan TR (2010) Relationship between historical sea-surface temperature variability and climate change-induced coral mortality in the western Indian Ocean. Marine Pollution Bulletin 60:964–970

Bahr KD, Jokiel PL, Rodgers KS (2016) Influence of solar irradiance on underwater temperature recorded by temperature loggers on coral reefs. Limnology and Oceanography: Methods 14:338–342

Baker-Médard M, Kroger E (2024) Troubling the Waters: Gendered Dispossession, Violence, and Sea Cucumber Aquaculture in Madagascar. Society & Natural Resources 37:443–470

Bos JT, Pinsky ML (2025) Fine resolution satellite sea surface temperatures capture the conditions experienced by corals at monthly but not daily timescales. Coral Reefs 44:423–434

Brown KT, Eyal G, Dove SG, Barott KL (2022) Fine-scale heterogeneity reveals disproportionate thermal stress and coral mortality in thermally variable reef habitats during a marine heatwave. Coral Reefs

Brown KT, Martynek MP, Barott KL (2024) Local habitat heterogeneity rivals regional differences in coral thermal tolerance. Coral Reefs

Bruggemann J, Rodier M, Guillaume M, Andréfouët S, Arfi R, Cinner J, Pichon M, Ramahatratra F, Rasoamanendrika F, Zinke J, McClanahan T (2012) Wicked Social-Ecological Problems Forcing Unprecedented Change on the Latitudinal Margins of Coral Reefs: the Case of Southwest Madagascar. Ecology and Society 17:

Buckee J, Hetzel Y, Edge W, Verduin J, Pattiaratchi C (2022) Daily timing of low tide drives seasonality in intertidal emersion mortality risk. Frontiers in Marine Science 9:

Buckee J, Pattiaratchi C, Verduin J (2020) Partial mortality of intertidal corals due to seasonal daytime low water levels at the Houtman Abrolhos Islands. Coral Reefs 39:537–543

Carter AL, Gilchrist H, Dexter KG, Gardner CJ, Gough C, Rocliffe S, Wilson AMW (2022) Cyclone Impacts on Coral Reef Communities in Southwest Madagascar. Front Mar Sci 9:

Castillo KD, Lima FP (2010) Comparison of in situ and satellite-derived (MODIS-Aqua/Terra) methods for assessing temperatures on coral reefs. Limnology and Oceanography: Methods 8:107–117

Castrillón-Cifuentes AL, Lozano-Cortés DF, Zapata FA (2017) Effect of short-term subaerial exposure on the cauliflower coral, Pocillopora damicornis, during a simulated extreme low-tide event. Coral Reefs 36:401–414

Chevalier C, Devenon J-L, Rougier G, Blanchot J (2015) Hydrodynamics of the Toliara Reef Lagoon (Madagascar): Example of a Lagoon Influenced by Waves and Tides. coas 31:1403–1416

Cinner JE, Bodin Ö (2010) Livelihood Diversification in Tropical Coastal Communities: A Network-Based Approach to Analyzing 'Livelihood Landscapes.' PLoS ONE 5:e11999

Cinner JE, Caldwell IR, Thiault L, Ben J, Blanchard JL, Coll M, Diedrich A, Eddy TD, Everett JD, Folberth C, Gascuel D, Guiet J, Gurney GG, Heneghan RF, Jägermeyr J, Jiddawi N, Lahari R, Kuange J, Liu W, Maury O, Müller C, Novaglio C, Palacios-Abrantes J, Petrik CM, Rabearisoa A, Tittensor DP, Wamukota A, Pollnac R (2022) Potential impacts of climate change on agriculture and fisheries production in 72 tropical coastal communities. Nat Commun 13:3530

Cinner JE, McClanahan TR, Graham NAJ, Daw TM, Maina J, Stead SM, Wamukota A, Brown K, Bodin Ö (2012) Vulnerability of coastal communities to key impacts of climate change on coral reef fisheries. Global Environmental Change 22:12–20

Cochrane KL, Rakotondrazafy H, Aswani S, Chaigneau T, Downey-Breedt N, Lemahieu A, Paytan A, Pecl G, Plagányi E, Popova E, van Putten EI, Sauer WHH, Byfield V, Gasalla MA, van Gennip SJ, Malherbe W, Rabary A, Rabearisoa A, Ramaroson N, Randrianarimanana V, Scott L, Tsimanaoraty PM (2019) Tools to Enrich Vulnerability Assessment and Adaptation Planning for Coastal Communities in Data-Poor Regions: Application to a Case Study in Madagascar. Frontiers in Marine Science 5:

Colin PL, Johnston TMS (2020) Measuring Temperature in Coral Reef Environments: Experience, Lessons, and Results from Palau. Journal of Marine Science and Engineering 8:680

660 Cullen-Unsworth LC, Nordlund LM, Paddock J, Baker S, McKenzie LJ, Unsworth RKF (2014)
661 Seagrass meadows globally as a coupled social–ecological system: Implications for
662 human wellbeing. Marine Pollution Bulletin 83:387–397

663 Cyronak T, Takeshita Y, Courtney TA, DeCarlo EH, Eyre BD, Kline DI, Martz T, Page H, Price
664 NN, Smith J, Stoltenberg L, Tresguerres M, Andersson AJ (2020) Diel temperature and
665 pH variability scale with depth across diverse coral reef habitats. Limnology and
666 Oceanography Letters 5:193–203

667 D'Agata S, Maina JM (2022) Climate change reduces the conservation benefits of tropical
668 coastal ecosystems. One Earth 5:1228–1238

669 Davis KA, Lentz SJ, Pineda J, Farrar JT, Starczak VR, Churchill JH (2011) Observations of the
670 thermal environment on Red Sea platform reefs: a heat budget analysis. Coral Reefs
671 30:25–36

672 De Frenne P, Beugnon R, Klinges D, Lenoir J, Niittynen P, Pincebourde S, Senior RA, Aalto J,
673 Chytrý K, Gillingham PK, Greiser C, Gril E, Haesen S, Kearney M, Kopecký M, le Roux
674 PC, Luoto M, Maclean I, Man M, Penczykowski R, van den Brink L, Van de Vondel S,
675 De Pauw K, Lembrechts JJ, Kemppinen J, Van Meerbeek K (2025) Ten practical
676 guidelines for microclimate research in terrestrial ecosystems. Methods in Ecology and
677 Evolution 16:269–294

678 Denny MW, Paine RT (1998) Celestial Mechanics, Sea-Level Changes, and Intertidal Ecology.
679 The Biological Bulletin 194:108–115

680 Drury C (2020) Resilience in reef-building corals: The ecological and evolutionary importance of
681 the host response to thermal stress. Molecular Ecology 29:448–465

682 Egbert GD, Erofeeva SY (2002) Efficient Inverse Modeling of Barotropic Ocean Tides. J Atmos
683 Oceanic Technol 19:183–204

684 European Union-Copernicus Marine Service (2016) Global Ocean 1/12° Physics Analysis and
685 Forecast updated Daily.

686 Farquhar S, Nirindrainy AF, Heck N, Saldarriaga MG, Xu Y (2022) The impacts of long-term
687 changes in weather on small-scale fishers' available fishing hours in Nosy Barren,
688 Madagascar. Front Mar Sci 9:

689 Fattebert C (2020) La pêche traditionnelle ou petite pêche maritime à Madagascar. 46

690 Fröcklin S, Torre-Castro M de la, Håkansson E, Carlsson A, Magnusson M, Jiddawi NS (2014)
691 Towards Improved Management of Tropical Invertebrate Fisheries: Including Time
692 Series and Gender. PLOS ONE 9:e91161

693 Gilman SE, Harley CDG, Strickland DC, Vanderstraeten O, O'Donnell MJ, Helmuth B (2006)
694 Evaluation of effective shore level as a method of characterizing intertidal wave
695 exposure regimes. Limnology & Ocean Methods 4:448–457

696 Glynn PW (1968) Mass mortalities of echinoids and other reef flat organisms coincident with
697 midday, low water exposures in Puerto Rico. Marine Biol 1:226–243

698 Glynn PW (1976) Some Physical and Biological Determinants of Coral Community Structure in
699 the Eastern Pacific. Ecological Monographs 46:431–456

700 Godefroid M, Vandendriessche M, Todinanahary GGB, Ransquin I, Dubois P (2024) Thermal
701 sensitivity of black corals (Antipatharia: Hexacorallia): Comparisons between sympatric
702 species from a thermally fluctuating site in Madagascar and between allopatric
703 congenerics. Science of The Total Environment 908:168311

704 Gough CLA, Dewar KM, Godley BJ, Zafindranosy E, Broderick AC (2020) Evidence of
705 Overfishing in Small-Scale Fisheries in Madagascar. Front Mar Sci 7:

706 Grantham R, Álvarez-Romero JG, Mills DJ, Rojas C, Cumming GS (2021) Spatiotemporal
707 determinants of seasonal gleaning. People and Nature 3:376–390

708 Guadayol Ò, Silbiger NJ, Donahue MJ, Thomas FIM (2014) Patterns in Temporal Variability of
709 Temperature, Oxygen and pH along an Environmental Gradient in a Coral Reef. PLOS
710 ONE 9:e85213

711 Harborne AR (2013) The ecology, behaviour and physiology of fishes on coral reef flats, and the
712 potential impacts of climate change. Journal of Fish Biology 83:417–447

713 Harley CDG, Helmuth BST (2003) Local- and regional-scale effects of wave exposure, thermal
714 stress, and absolute versus effective shore level on patterns of intertidal zonation.
715 Limnology & Oceanography 48:1498–1508

716 Harrington LJ, Otto FEL (2020) Reconciling theory with the reality of African heatwaves. Nat
717 Clim Chang 10:796–798

718 Harris A, Manahira G, Sheppard A, Gough C, Sheppard C (2010) Madagascar's Once Great
719 Barrier Reef – Change In Coral Reef Condition Over 40 Years.

720 Helmuth B, Yamane L, Lalwani S, Matzelle A, Tockstein A, Gao N (2011) Hidden signals of
721 climate change in intertidal ecosystems: What (not) to expect when you are expecting.
722 Journal of Experimental Marine Biology and Ecology 400:191–199

723 Herinirina PA, Bigot L, Frouin P, Volandrae HTE, Randriatsara RM, Behivoke F, Ranivoarivelo
724 L, Léopold M (2023) Seagrass macroinvertebrate bycatches support mosquito net trawl
725 fishery in Madagascar. Aquat Living Resour 36:18

726 Huang B, Liu C, Banzon V, Freeman E, Graham G, Hankins B, Smith T, Zhang H-M (2021)
727 Improvements of the Daily Optimum Interpolation Sea Surface Temperature (DOISST)
728 Version 2.1. Journal of Climate 34:2923–2939

729 Jankowski MW, Gardiner NR, Jones GP (2015) Depth and reef profile: effects on the distribution
730 and abundance of coral reef fishes. Environ Biol Fish 98:1373–1386

731 Jimenez IM, Kühl M, Larkum AWD, Ralph PJ (2008) Heat budget and thermal
732 microenvironment of shallow-water corals: Do massive corals get warmer than
733 branching corals? Limnology and Oceanography 53:1548–1561

734 Kearney MR (2006) Habitat, environment and niche: what are we modelling? Oikos 115:186–
735 191

736 Kekuewa SAH, Courtney TA, Cyronak T, Kindeberg T, Eyre BD, Stoltenberg L, Andersson AJ
737 (2021) Temporal and Spatial Variabilities of Chemical and Physical Parameters on the
738 Heron Island Coral Reef Platform. Aquat Geochem 27:241–268

739 Klinges DH, Duffy JP, Kearney MR, Maclean IMD (2022) mcera5: Driving microclimate models
740 with ERA5 global gridded climate data. Methods in Ecology and Evolution 13:1402–1411

741 Lachs L, Bozec Y-M, Bythell JC, Donner SD, East HK, Edwards AJ, Golbuu Y, Gouezo M,
742 Guest JR, Humanes A, Riginos C, Mumby PJ (2024) Natural selection could determine
743 whether Acropora corals persist under expected climate change. Science 0:eadl6480

744 Lavitra T, Vaïtilingon D, Rasolofonirina R, Eeckhaut I (2006) Seasonal abundance of sea
745 cucumber larvae at Toliara Great Reef, Madagascar. SPC Beche-de-mer Information
746 Bulletin 24:35–38

747 Le Manach F, Gough C, Harris A, Humber F, Harper S, Zeller D (2012) Unreported fishing,
748 hungry people and political turmoil: the recipe for a food security crisis in Madagascar?
749 Marine Policy 36:218–225

750 Le Nohaïc M, Ross CL, Cornwall CE, Comeau S, Lowe R, McCulloch MT, Schoepf V (2017)
751 Marine heatwave causes unprecedented regional mass bleaching of thermally resistant
752 corals in northwestern Australia. Sci Rep 7:14999

753 Leichter JJ, Deane GB, Stokes MD (2005) Spatial and Temporal Variability of Internal Wave
754 Forcing on a Coral Reef. Journal of Physical Oceanography 35:1945–1962

755 Lemahieu A, Scott L, Malherbe WS, Mahatante PT, Randrianarimanana JV, Aswani S (2018)
756 Local perceptions of environmental changes in fishing communities of southwest
757 Madagascar. Ocean & Coastal Management 163:209–221

758 Lima FP, Wethey DS (2012) Three decades of high-resolution coastal sea surface temperatures
759 reveal more than warming. Nat Commun 3:

760 Maka O, Pascal B, Todinanahary G (2022) Wild sea cucumber fishery in southwestern
761 Madagascar. SPC Beche-de-mer Information Bulletin 42:36–45

762 Margaritis G, Kent EC, Foster GL (2025) Intercomparison of satellite-derived SST with logger
763 data in the Caribbean—Implications for coral reef monitoring. PLOS Climate 4:e0000480

764 Mawren D, Hermes J, Reason CJC (2022) Marine heatwaves in the Mozambique Channel. Clim
765 Dyn 58:305–327

766 McClanahan TR, Ateweberhan M, Omukoto J, Pearson L (2009) Recent seawater temperature
767 histories, status, and predictions for Madagascar's coral reefs. Mar Ecol Prog Ser
768 380:117–128

McVean AR, Hemery G, Walker RCJ, Ralisaona BLR, Fanning E (2005) Traditional sea cucumber fisheries in southwest Madagascar: A case-study of two villages in 2002. SPC Beche-de-mer Information Bulletin 15–19

Medina-Valmaseda AE, Rodríguez-Martínez RE, Alvarez-Filip L, Jordan-Dahlgren E, Blanchon P (2020) The role of geomorphic zonation in long-term changes in coral-community structure on a Caribbean fringing reef. PeerJ 8:e10103

Mejía-Rentería JC, Castellanos-Galindo GA, Osorio-Cano JD, Casella E (2020) Subaerial exposure of coral reefs during spring low tides in the eastern Pacific. bms 96:219–220

Moustapha S, Chevalier C, Sow B, Pagano M, Devenon J-L (2021) Coupled effects of tide and swell on water renewal in a meso-tidal channel lagoon: Case of the Toliara Lagoon (Madagascar). Estuarine, Coastal and Shelf Science 259:107463

Obura D, Gudka M, Samoilys M, Osuka K, Mbugua J, Keith DA, Porter S, Roche R, van Hooidonk R, Ahamada S, Araman A, Karisa J, Komakoma J, Madi M, Ravinia I, Razafindrainibe H, Yahya S, Zivane F (2022) Vulnerability to collapse of coral reef ecosystems in the Western Indian Ocean. Nat Sustain 5:104–113

Pichon M (1978) Recherches sur les peuplements a dominance des anthozoaires dans les recifs coralliens de Tulear. 490

Rabesandratana H (1985) Sur quelques utilisations récifales à Madagsacar. Fifth International Reef Congress 6:661–668

Ranaivomanana HS, Jaquemet S, Ponton D, Behivoke F, Randriatsara RM, Mahafina J, Léopold M (2023) Intense pressure on small and juvenile coral reef fishes threatens fishery production in Madagascar. Fisheries Management and Ecology 30:494–506

Randrianarivo M, Botosoamananto RL, Guilhaumon F, Penin L, Todinanahary G, Adjeroud M (2023) Effects of Madagascar marine reserves on juvenile and adult coral abundance, and the implication for population regulation. Marine Environmental Research 190:106080

Randrianarivo M, Guilhaumon F, Tsilavonarivo J, Razakandrainy A, Philippe J, Botosoamananto RL, Penin L, Todinanahary G, Adjeroud M (2022) A contemporary baseline of Madagascar's coral assemblages: Reefs with high coral diversity, abundance, and function associated with marine protected areas. PLOS ONE 17:e0275017

Rasolofonirina R, Conand C (1998) L'exploitation des holothuries dans le sud-ouest de Madagascar, région de Toliarapar. SPC Beche-de-mer Information Bulletin 10:

Reid EC, Lentz SJ, DeCarlo TM, Cohen AL, Davis KA (2020) Physical Processes Determine Spatial Structure in Water Temperature and Residence Time on a Wide Reef Flat. Journal of Geophysical Research: Oceans 125:e2020JC016543

Rich WA, Glanz JS, Mele G, Burt NJ, Carvalho S, Doo SS, Goergen EA, Krieger EC, Li L, Osman EO, Suggett DJ, Johnson MD, Fox MD (2024) Widespread inconsistency in

logger deployment methods in coral reef studies may bias perceptions of thermal regimes. PLOS Climate 3:e0000517

Rivest EB, Gouhier TC (2015) Complex Environmental Forcing across the Biogeographical Range of Coral Populations. PLOS ONE 10:e0121742

Roesch A, Schmidbauer H (2018) WaveletComp: Computational Wavelet Analysis.

Schoepf V, Jung MU, McCulloch MT, White NE, Stat M, Thomas L (2020) Thermally Variable, Macrotidal Reef Habitats Promote Rapid Recovery From Mass Coral Bleaching. Front Mar Sci 7:

Schoepf V, Stat M, Falter JL, McCulloch MT (2015) Limits to the thermal tolerance of corals adapted to a highly fluctuating, naturally extreme temperature environment. Sci Rep 5:17639

Skirving W, Marsh B, De La Cour J, Liu G, Harris A, Maturi E, Geiger E, Eakin CM (2020) CoralTemp and the Coral Reef Watch Coral Bleaching Heat Stress Product Suite Version 3.1. Remote Sensing 12:3856

Sorte CJB, Bernatchez G, Mislan KAS, Pandori LLM, Silbiger NJ, Wallingford PD (2018) Thermal tolerance limits as indicators of current and future intertidal zonation patterns in a diverse mussel guild. Mar Biol 166:6

Stiepani J, Sandig A, Blicharska M (2023) The *Where*, the *How*, and the *Why* of the gleaning fishery: Livelihoods, food security, threats and management on the island of Malalison, Philippines. Ocean & Coastal Management 244:106806

Sutterley T, Alley K, Bishop-Taylor R, Brunt K, Howard S, Padman L, Siegfried M (2024) pyTMD.

Thompson AM, Stathakopoulos A, Hollister KJ, Lynch AM, Holder JC, Kuffner IB (2025) Acute heat stress and the extirpation of a threatened coral species from a remote, subtropical reef system. Coral Reefs

Thoral F, Montie S, Thomsen MS, Tait LW, Pinkerton MH, Schiel DR (2022) Unravelling seasonal trends in coastal marine heatwave metrics across global biogeographical realms. Sci Rep 12:7740

Tilley A, Burgos A, Duarte A, dos Reis Lopes J, Eriksson H, Mills D (2021) Contribution of women's fisheries substantial, but overlooked, in Timor-Leste. Ambio 50:113–124

de la Torre-Castro M, Fröcklin S, Börjesson S, Okupnik J, Jiddawi NS (2017) Gender analysis for better coastal management – Increasing our understanding of social-ecological seascapes. Marine Policy 83:62–74

Wallner-Hahn S, Dahlgren M, de la Torre-Castro M (2022) Linking seagrass ecosystem services to food security: The example of southwestern Madagascar's small-scale fisheries. Ecosystem Services 53:101381

Westerman K, Benbow S (2013) The role of women in community-based small-scale fisheries management: the case of the southern Madagascar octopus fishery. Western Indian Ocean Journal of Marine Science 12:119–132

White ER, Baker-Médard M, Vakhitova V, Farquhar S, Ramaharitra TT (2022) Distant water industrial fishing in developing countries: A case study of Madagascar. Ocean & Coastal Management 216:105925

White ER, Wulfing S (2024) Extreme events and coupled socio-ecological systems. Ecological Modelling 495:110786

Willer DF, Aldridge DC, Gough C, Kincaid K (2023) Small-scale octopus fishery operations enable environmentally and socioeconomically sustainable sourcing of nutrients under climate change. Nat Food 1–11

Woodson CB, Micheli F, Boch C, Al-Najjar M, Espinoza A, Hernandez A, Vázquez-Vera L, Saenz-Arroyo A, Monismith SG, Torre J (2019) Harnessing marine microclimates for climate change adaptation and marine conservation. Conservation Letters 12:e12609

Wulfing S, White ER (2024) Social-ecological models with social hierarchy and spatial structure applied to small-scale fisheries. Theor Ecol 17:325–336

Yamaguchi M (1975) Sea Level Fluctuations and Mass Mortalities of Reef Animals in Guam, Mariana Islands. 11:

Zafimahatradraibe JA, Ranaivomanana LNJ, Rakotomahazo C, Randriamanantsoa B, Hartmann AC, Todinanahary GGB (2025) Authority, capacity, and power to govern: Three marine protected areas co-managed by resource users and non-governmental organizations. Marine Policy 177:106647

Zhang Z, Falter J, Lowe R, Ivey G, McCulloch M (2013) Atmospheric forcing intensifies the effects of regional ocean warming on reef-scale temperature anomalies during a coral bleaching event. Journal of Geophysical Research: Oceans 118:4600–4616

Supplemental Material

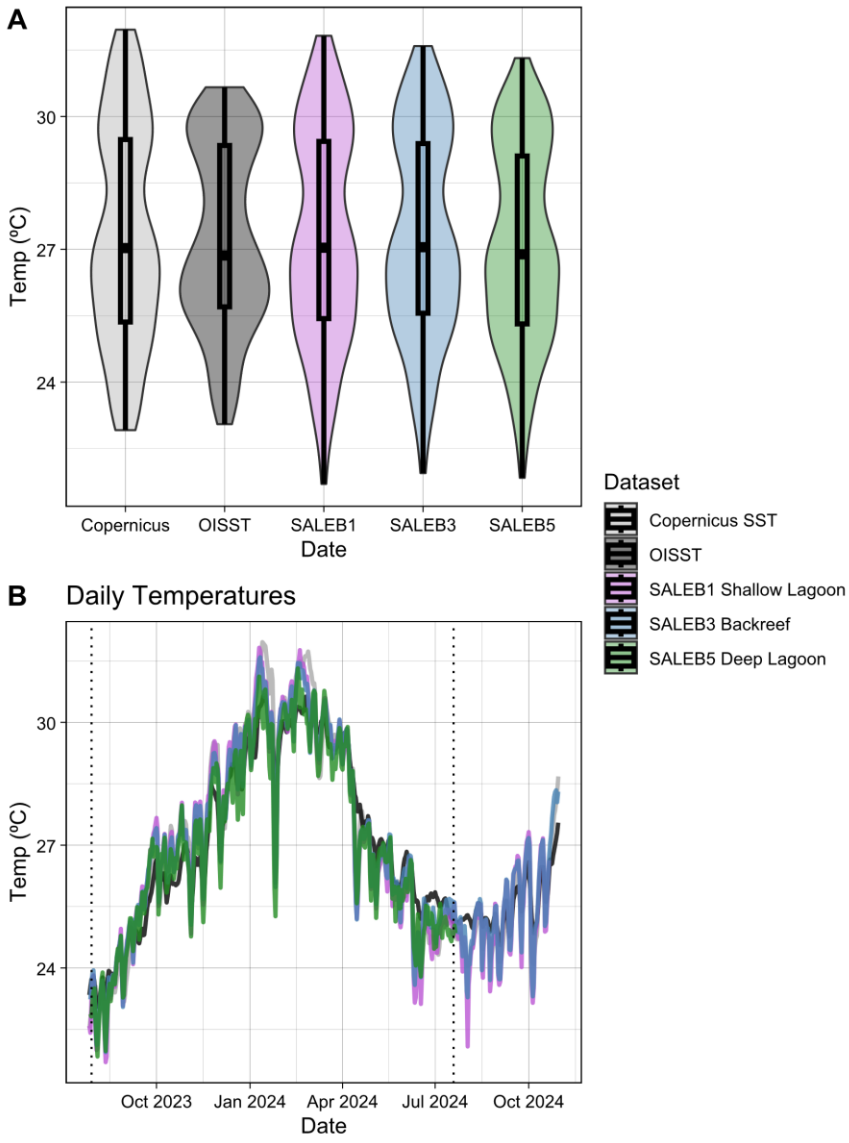

Supplementary Figure 1 A-B comparison of remote-sensed sea water temperature products (Copernicus SST, NOAA OISST) and *in-situ* reef temperature recorded using loggers, with data summarized as daily means. Logger temperatures were recorded every 15 minutes, so we summarized temperatures as a daily mean to compare them to gridded reanalysis temperature products, which interpolate sea water temperature on a daily time step. OISST records sea surface temperatures, while Copernicus interpolates temperatures at a 0.5 m depth. Pairwise multiple comparisons revealed no statistical significance between any two sites. Dashed vertical lines in **B** indicate the extent of data used for cross-site comparisons.

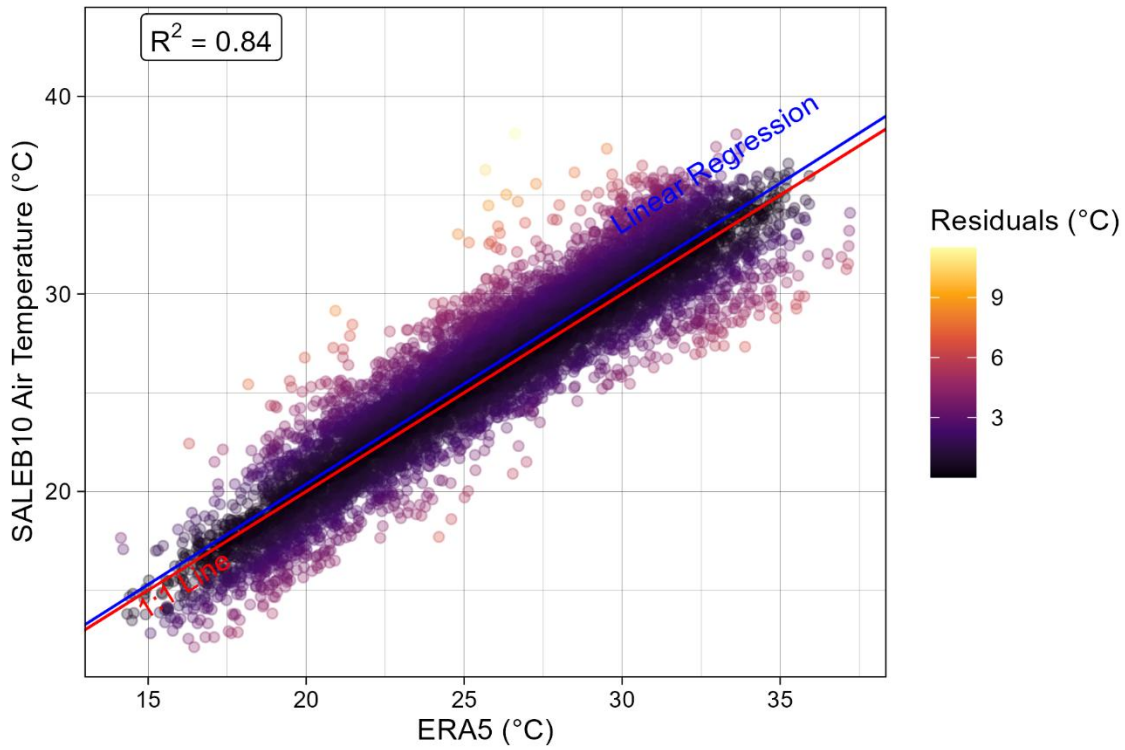

Supplementary Figure 2 Correlation plot between ERA5 2 m air temperatures and logger air temperatures in Salary village. The red line indicates a 1:1 line, and the blue line indicates the linear regression of the data. Note that large positive residual observations (>5 °C) are likely due to the logger being exposed to the direct sun.

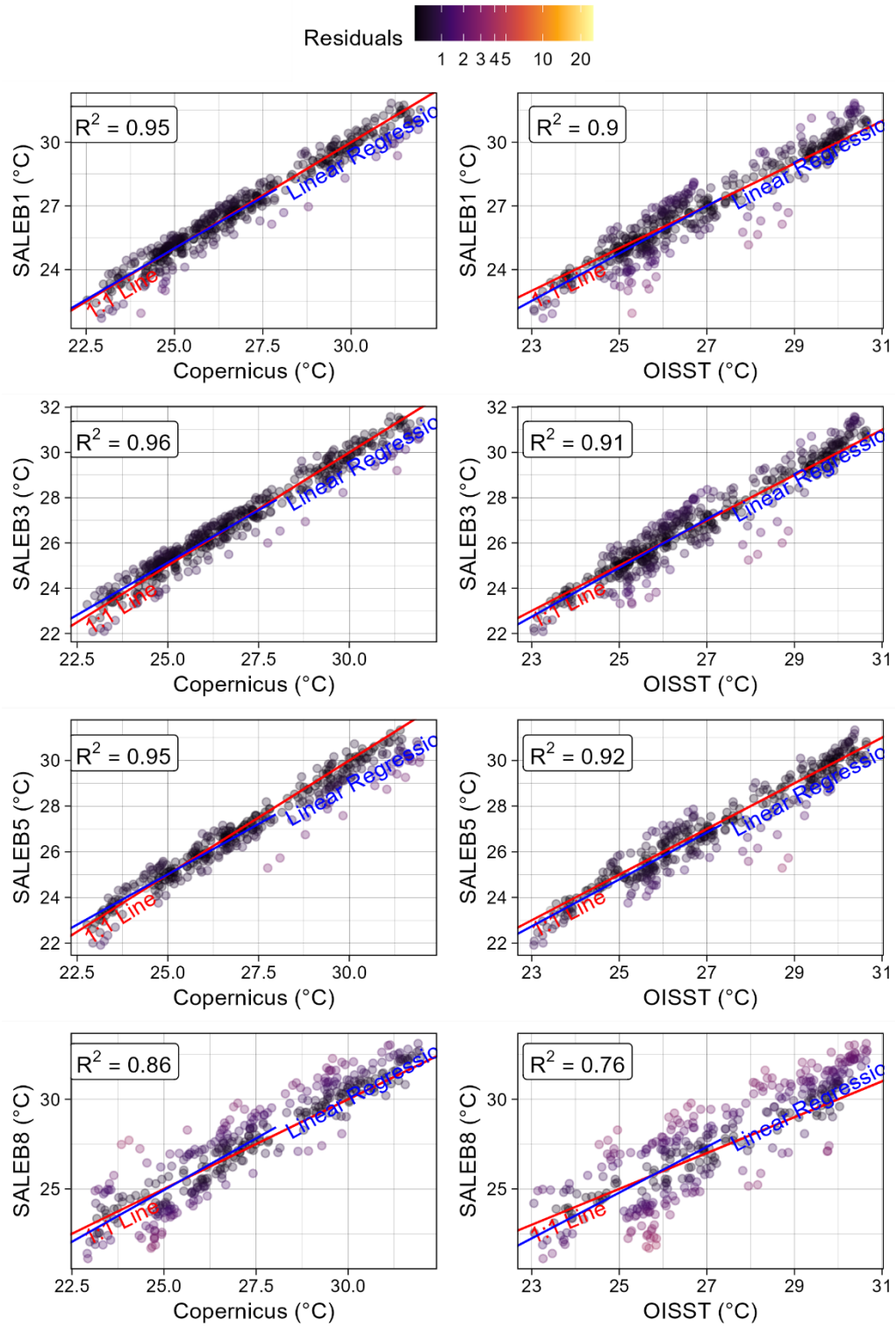

Supplementary Figure 3 Correlation plot between Copernicus and OISST sea surface temperature observations and summarized daily mean logger temperatures at Salary reef. The red line indicates a 1:1 line, and the blue line indicates the linear regression of the data. The color scale of the residuals is pseudo-log to accommodate the range of residuals between sites.

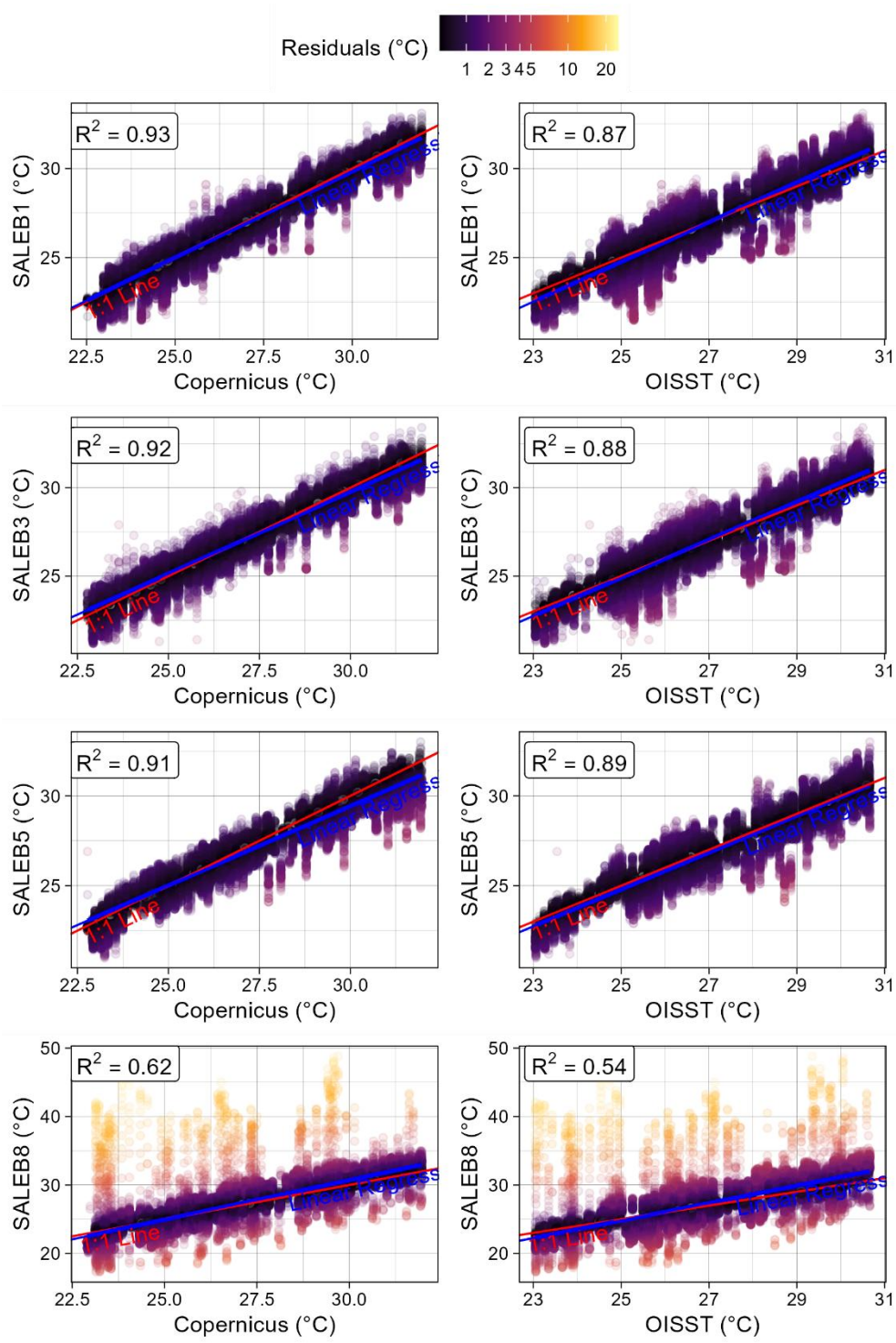

Supplementary Figure 4 Correlation plot between Copernicus and OISST sea surface temperature observations and summarized raw logger temperatures (collected every 15 minutes) at Salary reef. The red line indicates a 1:1 line, and the blue line indicates the linear regression of the data. The color scale of the residuals is pseudo-log to accommodate the range of residuals between sites.

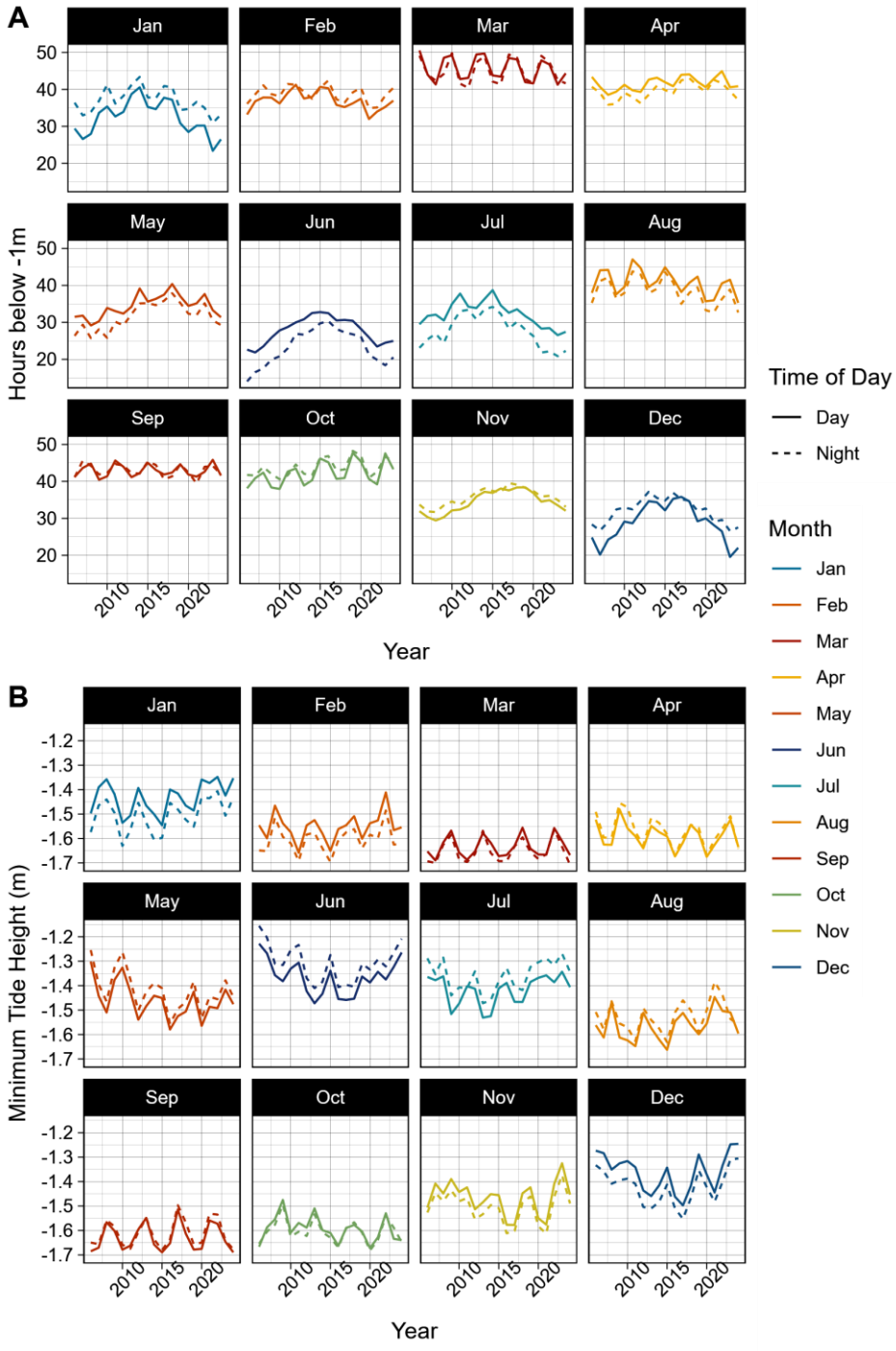

902

903 **Supplementary Figure 5 A** Hours spent below -1 m (mean tide, TPXO9 tide model) and **B**
904 minimum tide height (TPOX9 tide model) across 19 years, by month and time of day, on Salary
905 Reef. Months are color-coded based on the maximum temperature from our intertidal flat
906 temperature logger (SALEB8) for each month during the observation period (2023-2024), with
907 red equaling the warmest and blue equaling the coldest.

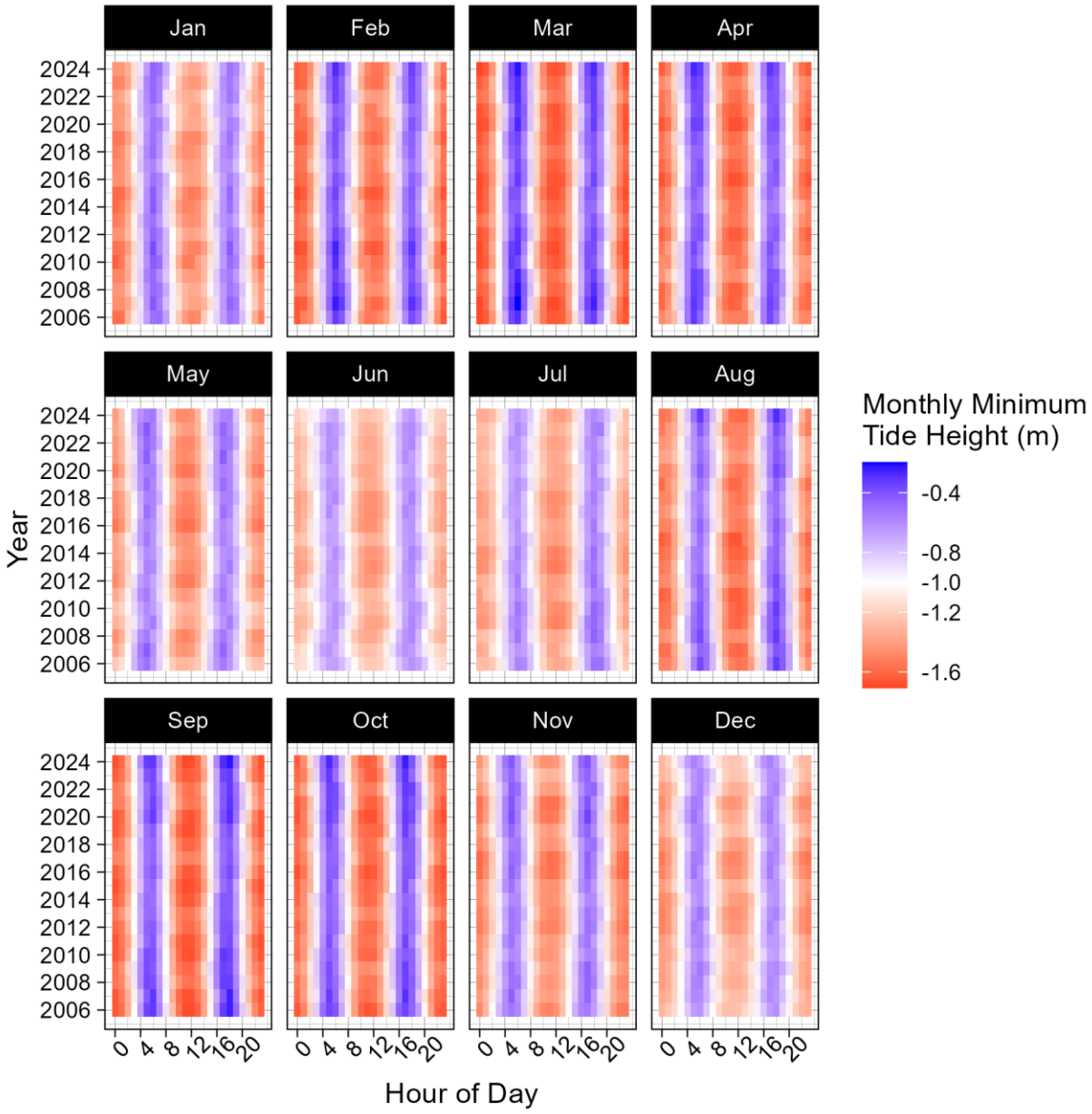

908

909 **Supplementary Figure 6** Minimum tide height each month for a given hour of the day and year
910 at Salary reef (TPXO9 tide model). Low tides that exceeded -1 m consistently occur between
911 09:00 and 15:00.

912

913

914

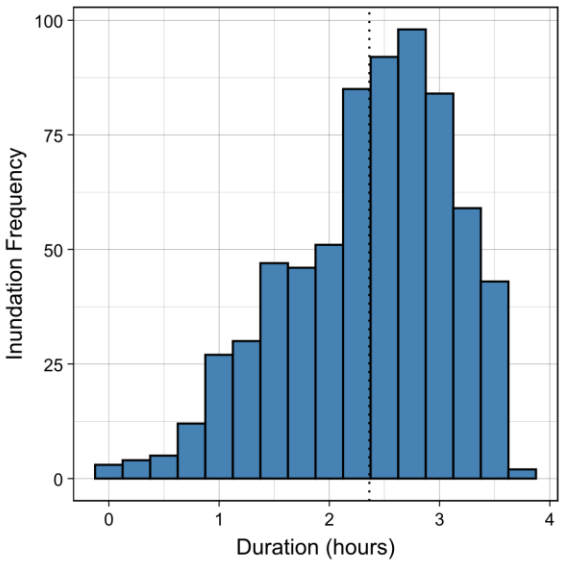

Supplementary Figure 7 Histogram of intertidal logger (SALEB8) inundation duration at the interpolated tidal height (-0.96m). The dotted vertical line indicates the mean inundation duration of 2.36 hours.

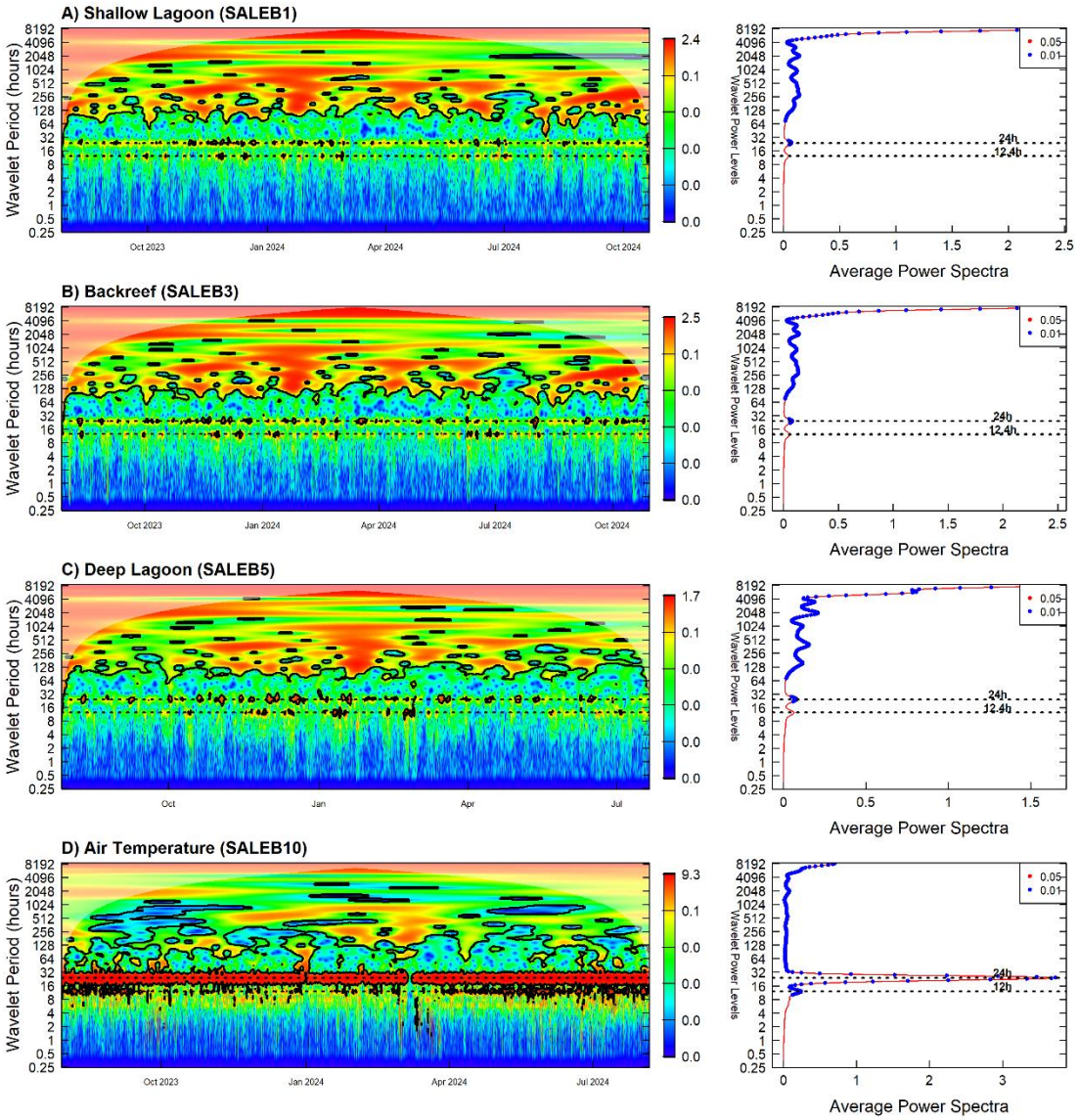

Supplementary Figure 8 Wavelet plots for the subtidal loggers (**A-C**) and air temperature logger (**D**). 24-hour horizontal lines indicate the position of power bands associated with daily solar cycles, while the 12.4-cycle corresponds with tidal cycles. The 12-hour cycle identified in the air temperature logger is likely due to semi-diurnal atmospheric tides and land-sea breeze circulation, which are strongest during cloudless seasons (warm-dry season). Black outlines in the wavelet plots indicate regions with pairs of dates/times and cycle periods that have strong power support ($p < 0.01$). Colored dots on the average wavelet plots indicate the strength of support for a significant wavelet period at a given duration.

Table S1 Site data for logger deployments at Salary reef. Of the ten total loggers deployed, we recovered five (four on the reef and one air temperature logger).

Logger ID	Latitude	Longitude	Approximate Depth (m)	Zone	Recovered Logger Code	Fishing Style	Deployment Date	Recovery Date	Days of Data
SALEB1	-22.5367	43.2566	3	Lagoon	Shallow Lagoon	boat	7/27/2023	10/22/2024	453
SALEB2	-22.5512	43.281017	2	Reef Flat		gleaning	7/28/2023		
SALEB3	-22.5343	43.24945	2	Backreef	Backreef	boat	7/28/2023	10/31/2024	461
SALEB4	-22.5367	43.2566	3	Lagoon		boat	7/28/2023		
SALEB5	-22.5387	43.2575	4	Lagoon	Deep Lagoon	boat	7/28/2023	7/22/2024	360

SALE B6	-22.5863	43.24875	2	Forereef		boat	7/28/2023		
SALE B7	-22.5863	43.24875	2	Forereef		boat	7/28/2023		
SALE B8	-22.553	43.281067	2	Reef Flat	Flat	gleaning	7/29/2023	7/20/2024	357
SALE B9	-22.5493	43.282483	2	Reef Flat		gleaning	8/10/2023		
SALE B10	-22.5542	43.285767		Air Temperature	Chez Fred		7/29/2023	8/7/2024	375

Supplement Text

To determine the immersion regime of the field intertidal temperature logger, we built a function to extract the tidal height of the logger and apply an interpolated time series of immersion/emersion status to the measured intertidal temperatures. We first identified logger immersion points, diagnostic as precipitous drops of at least 3 °C/15 min from temperature peaks that occur during summer low tide events (Harley and Helmuth 2003; Gilman et al. 2006). We manually extracted points that visually fit this drop criterion, as we found other peak-finding algorithms to misidentify smaller drops as immersion points.

To determine the immersion regime of the intertidal flat logger (SALEB8), we developed a custom R function, *tide_findR*, to estimate the local tide height and time offset from the interpolated tide series at -22.6° S, 43.25° E using the *pyTMD* python package (Egbert and Erofeeva 2002; Sutterley et al. 2024); see Methods. Since tidal height and timing can vary spatially, this adjustment was necessary to align logger immersion events with the local tidal cycle.

First, the function shifts the reference tide series forward in time, extracting tide heights corresponding to each recorded immersion timestamp. At each shift, the function calculates the sum of squared differences (least squares) between observed immersion heights and the mean tide height. The time offset that minimizes the least squares is selected as the best estimate of the logger's time shift relative to the reference tide station. While a single time offset may not precisely describe the complexities of water movement within a barrier reef system, this approach approximates the time difference between the open-ocean tide model and experienced tides close to shore, within the Salary reef lagoon.

Using this optimal time shift, the function assigns a tide height to each immersion timestamp and calculates a mean logger height, representing the submergence threshold. This threshold is

then used to classify each temperature observation as submerged (immersed) or exposed (emersed), providing a time series of temperature data linked to tidal exposure.

Supplement Citations

Egbert GD, Erofeeva SY (2002) Efficient Inverse Modeling of Barotropic Ocean Tides. J Atmos Oceanic Technol 19:183–204

Gilman SE, Harley CDG, Strickland DC, Vanderstraeten O, O'Donnell MJ, Helmuth B (2006) Evaluation of effective shore level as a method of characterizing intertidal wave exposure regimes. Limnology & Ocean Methods 4:448–457

Harley CDG, Helmuth BST (2003) Local- and regional-scale effects of wave exposure, thermal stress, and absolute versus effective shore level on patterns of intertidal zonation. Limnology & Oceanography 48:1498–1508

Sutterley T, Alley K, Bishop-Taylor R, Brunt K, Howard S, Padman L, Siegfried M (2024) pyTMD.